Environmental Science Nano

Rapid detection of nutrients with electronic sensors: a review

Journal:	*Environmental Science: Nano*
Manuscript ID	EN-CRV-12-2017-001160.R1
Article Type:	Critical Review
Date Submitted by the Author:	23-Feb-2018

Complete List of Authors:	Chen, Xiaoyan; Tongji University Zhou, Guihua; University of Wisconsin-Milwaukee, Mechanical Engineering Mao, Shun; Tongji University, College of Environmental Science and Engineering; University of Wisconsin, Milwaukee, Mechanical Engineering Chen, Junhong; University of Wisconsin-Milwaukee, Mechanical Engineering

Environmental significance

Determining nutrient levels is critical for evaluating water eutrophication and is an important water quality factor in waste water treatment and reclamation. Increasing demand for nutrient sensors with high sensitivity and selectivity, real-time monitoring, and in situ detection leads to many research studies on new sensing technologies. Electronic sensors that rely on electrical signals have shown outstanding properties and capabilities for low-level and rapid detection of nutrients. Nanomaterials, which are incorporated as the sensor's sensing element, can enhance sensor performance in terms of sensitivity and selectivity. Electronic sensing platforms provide field-deployable, real-time, inexpensive, and miniaturized sensors for monitoring nitrogen salts and phosphates in water. This will benefit the water industry, agriculture, and environmental regulators by providing accurate and accessible sensing capabilities for monitoring nutrients, leading to better evaluation and control of water quality.

Environmental Science Nano

CRITICAL REVIEW

Rapid detection of nutrients with electronic sensors: a review

Xiaoyan Chen,[†ab] Guihua Zhou,[†c] Shun Mao*[ab] and Junhong Chen*[c]

Received 00th January 20xx,
Accepted 00th January 20xx

DOI: 10.1039/x0xx00000x

www.rsc.org/

Nutrients such as nitrogen and phosphorus are key indexes in evaluating water eutrophication. Electronic sensors, *i.e.*, potentiometric sensors, voltammetric sensors, and field-effect transistor (FET) sensors, that rely on electrical signals (*e.g.*, potential, current and resistance) have shown unique properties and capabilities in detecting nutrients. Compared with conventional methods, these electronic sensors enable a rapid and low-level detection of nitrogen salts and phosphates in water. Over the past decades various sensor designs and sensing elements have been studied and reported. With the development of nanomaterials, the performance of electronic sensors has been further improved, presenting tremendous opportunities for detecting nutrients and other water contaminants. This review article will introduce the recent progress of electronic sensors in detecting nitrogen salts and phosphates, and will discuss current limitations and future directions for these sensors.

1. Introduction

Nutrients such as nitrate, nitrite, ammonium, and phosphate play a vital role for living organisms in aquatic ecosystems and water environments. However, even a modest increase in nutrients can, under the right conditions, set off a whole chain of undesirable events in a water environment, including accelerated plant growth, algae blooms, low dissolved oxygen, and the death of fish and other aquatic animals, known as eutrophication. Therefore, the level of nutrients in water should be closely monitored to protect rivers, streams, and reservoirs. Spectroscopy and chromatography are standard and conventional methods for detecting nutrients;[1-3] however, they are limited by relatively low sensitivity and the need chemical reagents for detection, and thus they are not suitable for real-time and online nutrient detection. With the increasing demand for field-deployable, rapid, sensitive, and inexpensive sensors, electronic nutrient sensors have been widely studied over the past decades.

Potentiometric sensors, voltammetric sensors, and field-effect transistor (FET) sensors are three representative electronic sensors for detecting nutrients. Different from conventional sensors, the electronic sensors provide unique superiority. For instance, electronic sensors convert chemical signals directly into electrical signals without sample pretreatment and post-processing, providing simple sensor operation and signal acquisition. Moreover, by using nanomaterials, *e.g.*, one-dimensional (1D) and two-dimensional (2D) nanomaterials, as the sensing element or sensor electrode, the sensing performance of electronic sensors has been significantly improved in the last decade. Therefore, due to their unique structures and outstanding performance, electronic sensors show great promise for nutrient detection, offering high sensitivity, high selectivity, and rapid response. Previous reviews on nutrient detection typically focus on various detection methods, including spectroscopy, chromatography, and electronic sensors;[4-12] however, no review article has emphasized the significance of rapid detection or the low-level detection of nutrients in water systems. Although some reviews focus on electronic sensors for detecting nutrients,[13-17] they separately focus on nitrate,[13, 14] nitrite,[13, 15] or phosphate.[16, 17] Moreover, as an emerging sensing platform, FET sensors have been reported for nutrient detection with high potential in low concentration levels and real-time detection, which has not been reviewed. This review article will discuss the recent progress of electronic sensors, including potentiometric sensors, voltammetric sensors, and FET sensors, for the rapid and low concentration detection of nutrients such as nitrogen salts and phosphate. This review will also evaluate perspectives on the future development of electronic sensors for detecting nutrients and other water contaminants, as well as the challenges facing electronic sensors in water quality monitoring.

2. Potentiometric sensors

Potentiometric sensors, which use ion selective electrodes (ISEs) as the sensing element, is one of the earliest and most frequently used sensors for detecting ions in solution. ISEs were intensely studied in the 1960s after several decades of development from the spherical glass membrane by Helmoholtz, which was based on

[a] *State Key Laboratory of Pollution Control and Resource Reuse, College of Environmental Science and Engineering, Tongji University, 1239 Siping Road, Shanghai 200092, China. E-mail: shunmao@tongji.edu.cn*
[b] *Shanghai Institute of Pollution Control and Ecological Security, Shanghai 200092, China*
[c] *Department of Mechanical Engineering, University of Wisconsin-Milwaukee, 3200 N. Cramer Street, Milwaukee, WI 53211, USA. E-mail: jhchen@uwm.edu*
[†] *These authors contributed equally to this work.*

Faraday's conception.[18] The early ISEs were used for testing H^+ ion,[19] followed by extended applications in other ions such as Na^+, Li^+, Ca^{2+}, Cl^-, Br^-, I^-, Mg^{2+}, and K^+. Rapid advancements in membrane, *e.g.*, from inorganic to organic, natural to synthetic, macro to nano, solid to liquid, has improved the performance of ISEs. Nowadays, polymers are one of the most commonly used membrane materials in ISE. For example, polyvinyl chloride (PVC) is widely applied as sensing membrane matrix,[20] while conducting polymers such as polypyrrole, polythiophene and polyaniline are used as ion-to-electron transducers in solid-contact ISEs for sensing applications.[21] Based on the ion exchange mechanism, ionophores were developed to facilitate the transfer of ions and to improve the selectivity of ISE. The first study to detect nutrients using a potentiometric sensor was reported by Stefanac and Simon, who used a neutral carrier membrane electrode to detect ammonium.[22] Since then, potentiometric sensors have been widely studied and applied to detect nitrate, nitrite, and phosphates, and they have shown a high capability for practical applications.

2.1 Device structure and working principle

Potentiometric sensing with ISE is a zero-current sensing technique that is based on the potential difference across an interface, often a membrane. The membrane is the key element of potentiometric sensor and it is made up of a certain ionophore or ion-exchanger, which attracts target ions or particular electroactive constituents and decides the sensitivity and specificity of the sensor. As shown in Fig. 1, a reference electrode (RE) immersed in the inner reference solution is used to offer a fixed inside surface potential of the membrane. The outside surface potential of the membrane is measured by an indicator electrode (*e.g.*, copper, platinum electrode). By measuring the difference between the inside and outside potentials of the membrane surface, the nutrient ions could be detected. Various materials have been used in the membrane, either solid-state or liquid-state. Some of the membranes (*e.g.*, osmosis, cell membranes) allow the ions to travel through while other membranes (*e.g.*, glass membranes) do not. Conventional ISEs are typically based on liquid contact (LC), and the sensing membrane is sandwiched between two solutions (the inner reference solution and the sample) during operation (Fig. 1a). Solid-contact (SC) ISEs are also used with a direct contact between the conducting wire and the membrane, in which the sensing membrane is sandwiched between the solid contact and the sample solution (Fig. 1b).

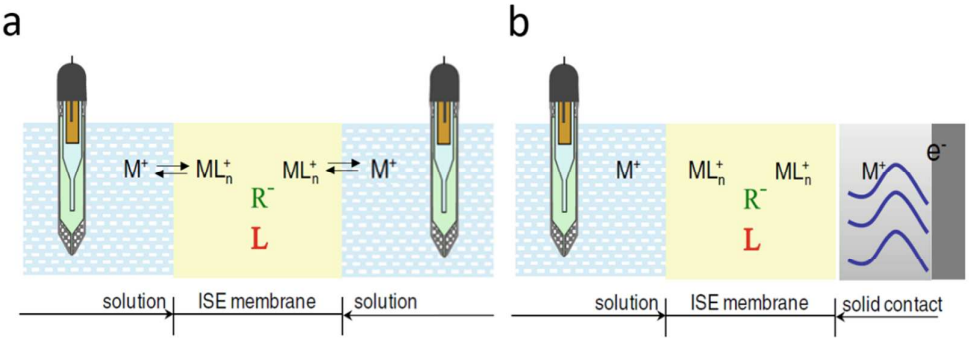

Fig. 1 Structure of potentiometric sensors: (a) liquid contact ISE and (b) solid contact ISE. Reproduced with permission from ref. [20]. Copyright 2009, Springer International Publishing AG.

While the sensing response is given from the external, the membrane potential is responsible for the sensing mechanism. The nature of potentiometric sensors is a galvanic cell in which the potential difference between two electrodes exists with no current flow. In the potentiometric sensor, the electromotive force of the cell is defined as the response of the sensor, stemming from the membrane potential. In the 1930s, a host of theories, including the sieving action principle, the fixed-charge principle, and the adsorption theory, had tried to explain the membrane potential.[23, 24] However, the most widely accepted theory revealing membrane potential was developed from the diffusion theory of electrolyte established by Nernst,[25, 26] which was based on the thermodynamics and electrolyte solution developed by Helmholtz, Gibbs, Boltzmann, van't Hoff and Arrhenius. As shown in Fig. 2, the membrane potential consists of two parts: the diffusion potential and Donnan potential. The membrane itself, or the ionophore immobilized in it, enables the ions to diffuse through the interphase between the sample solution and the membrane due to the concentration difference, forming an electric field perpendicular to the interface. Therefore, the diffusion potential is nonspecific to ions. In contrast, the Donnan potential is selective, because some ions in the membrane are fixed and relative movement exists inside the membrane but cannot move freely into sample solution. The ions that accumulate at one side of the interface contribute to the Donnan potential. Since the concentration of analytes in sample solution and inner solution are different, the potential on each side of the membrane are thus unequal, the difference of which is detected by an external circuit, and thus defines the membrane potential.

The value of the membrane potential is calculated as the difference between the interface potential on both sides of the membrane:

$$\varphi_{\mathrm{m}} = \varphi_{\mathrm{out}} - \varphi_{\mathrm{in}}, \quad (1)$$

where φ_m, φ_{out} and φ_{in} are the membrane potential, outside electrode potential, and inside electrode potential (RE potential),

respectively. Based on the Nernst equation and the theory of activity and activity coefficient, the electrode potential is deduced as:

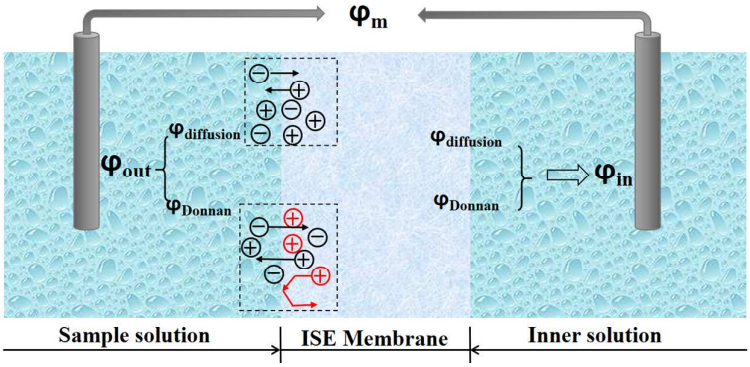

Fig. 2 Working mechanism of ISE: formation of membrane potential; inner: coefficient of the diffusion potential and the Donnan potential; external: the potential difference between the outer electrode and the inner reference electrode.

$$\varphi = \varphi^{\theta} + \frac{\mathrm{RT}}{z_i \mathrm{F}} \ln \alpha_{\mathrm{i}}, \quad (2)$$

where φ and φ^{θ} are the actual and standard potential, respectively, *R* is the gas constant, *T* is the temperature, *F* is the Faraday's constant, and z_i and α_i are the charge number and activity of the target ion (i), respectively. Combining equations (1) and (2), the potential response is obtained:

$$\varphi_{\mathrm{ISE}} = \varphi_{\mathrm{m}} = \mathrm{K} + \frac{\mathrm{RT}}{z_{\mathrm{i}} \mathrm{F}} \ln \alpha_i, \quad (3)$$

where *K* is a constant and can be explained as the standard potential of ISE, and α_i refers to the ion activity of samples (outside the membrane). Since α_i can be obtained by the measured φ_{ISE} from Equation (3), the concentration of the ions c_i then can be calculated from $\alpha_i = \gamma_i c_i$ (where γ_i is the activity coefficient).

The functionality of potentiometric sensors relies on the sensing membrane, which is a carrier that adsorbs target ions. For detecting nutrient ions, the current problems with potentiometric sensors include interference from other species, an inadequate lower detection limit, and difficulty with miniaturization. To improve the sensor performance, research on potentiometric nutrient sensors have mainly focus on new ISE material, *e.g.*, ionophore and its composites, as well as micro/nanomaterials.

2.2 Nitrogen salt detection

A potentiometric sensor for nitrogen salt was first reported by Stefanac and Simon in 1966. The sensor detected NH_4^+ using a neutral carrier (macrotetrolide antibiotics nonactin), which has good selectivity to NH_4^+ over K^+ and Na^+. Later on, ISEs for nitrate and nitrite detection were reported;[27, 28] however, ISEs for nitrogen salts are not widely used because of interfering ions and the concentrations of nitrogen salts in surface water are close to the detection limit of commercial ISEs. Therefore, to meet the requirements for surface-water sensing, recent studies on the potentiometric sensing of nitrogen salts focus more on selectivity and lower detection limits, both of which require revolutionary ISE materials.

Ammonium potentiometric sensors with classical ionophore (nonactin/NA) have a selectivity over K^+ but less than two orders of magnitude ($\log K_{NH_4^+,K^+} = -1.0$). Such selectivity is unsatisfactory for practical application, and thus more selective sensors were pursued for accurate detection of environmental samples considering the existence of K^+ in water. The improvement of NH_4^+ ISEs is mainly based on the structure modification of ionophores, *e.g.*, the anion additive and plasticizer. The recent boom of synthetic materials brings new vitality in the design of the NH_4^+ selective membrane. A novel ionophore with a superior NH_4^+ selectivity compared with natural antibiotic nonactin was successfully synthesized based on 19-membered crown compounds. Lehn *et al.* reported a spherical macrotricyclic cryptand whose selectivity of NH_4^+ over K^+ is 250 times higher than nonactin;[29] and Kim *et al.* reported thiazole-containing benzo-crown ethers as the ionophore with an enhanced selectivity for NH_4^+ over Na^+.[30]

ISE membranes can be fabricated with organic liquids and polymers. Particularly, PVC has attracted considerable attention due to its excellent properties such as permeability, plasticity, and ease of fabrication. PVC is suitable for ISE construction and is typically used as the matrix-immobilizing nonactin to fabricate the sensing membrane.[31-34] To enhance the sensor performance, various anionic additives were used with PVC. A 15-crown-5-functionalized carbosilane dendrimer was used as a ionophore carried by PVC and assisted by the addition of anion excluder sodium tetraphenyl borate, leading to a detection limit of 3.9 μM for NH_4^+.[35] Tetrakis (4-chlorophenyl) borate potassium salt and the plasticizer dioctyl sebacate were added to the PVC, achieving a detection limit as low as 2.2 μM.[36]

With the development of the ionophore and sensing membrane, solid-contact ISEs offer a new direction for ammonium potentiometric sensors. The selectivity of SC ISE can be improved by enzymes and conductivity enhancers due to the solid contact. For instance, Di-cyclo-hexyl-18-crown-6 and nonactin were used as an ionic conductivity enhancer and ionophore, respectively, together with a layer of creatininase, forming a composite SC ISE for NH_4^+ detection. This sensor shows a high sensitivity, a high selectivity, easy miniaturization, and multi-sensing implementations.[37] A bienzymatic potentiometric sensor was also prepared with SC ISEs based on carboxylated PVC matrix

membrane with urease and creatinase, which performed better than those of the PVCs containing traditional ionophores.[38]

Nanomaterials, due to their unique structures and properties, have been used in ion selective membranes to address the drawbacks of conventional solid transducers and conductive polymers. For example, side redox reactions may happen when using conductive polymers during sensing, as they are sensitive to light, oxygen, and carbon dioxide. Alternatively, nanomaterials, *e.g.*, carbon nanotube (CNT) and graphene, are more electrochemically and optically stable and have better conductivity, thereby leading to a better performance in the membrane. Moreover, porous nanostructures make it easy for ions to travel through; however, because of the difficulty in forming the matrix alone and the limited load capacity for macromolecular ionophores or enzymes, nanomaterials are often used in combination with polymers. For example, reduced graphene oxide was used by Ping *et al.* in SC ISE with a PVC-based selective membrane, showing an improved performance over that of conducting polymer-based sensors.[39] Recently, a nanomaterial-based ammonium sensor was reported by Robini *et al.* with a CNT/PVC-based membrane. Compared with the sensor that had a plasticizer-free methacrylate copolymer-based sensing layer, Robini *et al.* showed a similar lower limit of detection (LOD) for ammonium of 0.26 µM.[40] Silver/nano-silver wire, polyaniline, and poly(o-phenylenediamine) were also used as the substrate, transducer, and sensitive membrane, respectively, in an NH_4^+ SC ISE, which exhibited a quick response to NH_4^+ of 0.5-2 s with good sensitivity and selectivity.[41]

Nitrate ion is another important nutrient in water, and significant effort has been made to develop nitrate potentiometric sensors. The traditional NO_3^- ISE was based on a PVC membrane loading a nitrate selective ionophore, an ion-exchanger, and electrolyte. Until now, reported NO_3^- ISEs exhibited a good selectivity over interfering ions such as Cl^-, SO_4^{2-}, and SCN^- with selectivity coefficients as high as 1000 and an LOD down to 1 µM.[42, 43] Recent studies of nitrate potentiometric sensors have concentrated more on solid-contact ion selective electrodes because the filling solution is not required, they are more rugged, and it is easier to realize miniaturized construction. For instance, as shown in Fig. 3a-c,[42] three types of electrode structures were applied for nitrate detection. The nitrate potentiometric sensor comprised an all-solid-state nitrate selective electrode, which was based on a miniaturized reference electrode, an ion-to-electron transducer, and lipophilic multiwalled carbon nanotubes (f-MWCNTs). Three different membranes, acrylic membrane and PVC membranes with bis (2-ethylhexyl) phthalate (DEHP) and o-2-nitrophenyl octyl ether (o-NPOE) were tested, and the acrylic membrane showed an LOD of 0.09±0.01 µM. To prepare the sensor electrode, a mixture of carbon power (graphite) and a binder pasting liquid called carbon paste is commonly used. Various nitrate sensors were reported for their easy assembly and membrane modifications, with an LOD on the level of 1 µM.[44-47]

In recent years, conductive polymers, which have both advantages of conductor and polymer, are regarded as an ideal electrode membrane material because conductivity is necessary for the solid contact while the polymer network provides the capability for ionophore loading and modification. Electropolymerized polypyrrole with sodium nitrate supporting electrolyte has been used as the membrane matrix.[48-50] Later on, N-methyl pyrrole became an alternative due to its stable performance in a wider range of pH and a higher degree of branching and crosslinking (*i.e.*, improved selectivity because of the ionic imprinting).[51, 52]

Nanomaterials have also attracted much attention in nitrate ISE because of their unique mechanical and electrical properties. For example, platinum (Pt) nanoparticles (NPs),[53] CNTs,[54] and graphene[55] have been used in ISE and achieved good potential stability and capacity. Lipophilic carbon nanotubes were used as an ion-to-electron in solid-contact ISE, which exhibited an LOD down to 0.5 µM, and a rapid response within 5 s.[42] Different types of nanosized carbon black (CB) were added into the membrane substance plasticized PVC as a solid-contact nitrate ISE with a close-to Nerstian slope in the range from 10^{-1} to 10^{-6} M and stable potentials (LOD: 0.25 µM).[56]

Biomaterials, like biocatalysts nitrate reductase (NaR), were used as biological recognition elements with high specificity and efficiency to enhance the performance of NO_3^- ISEs by reducing the nitrate.[57] In these sensors, flavin adenine dinucleotide (FAD) and nicotinamide adenine dinucleotide (phosphate) (NAD(P)H) are the subunits, which undergo an oxidation/reduction process involving the Mo(VI)/Mo(IV) redox-coupled reaction and the reduction of nitrate to nitrite, respectively.[58-63] Bio-potentiometric sensors have been frequently used to replace the conventional ISEs because of their good specificity, simplicity, and low detection limit.

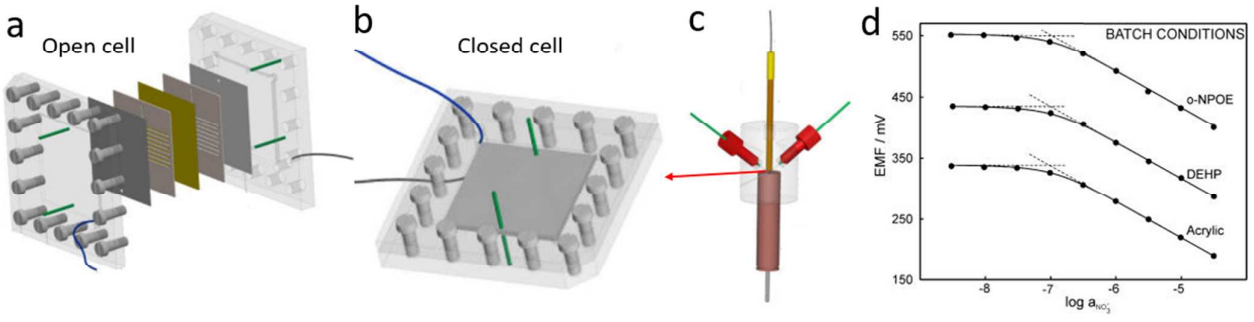

Fig. 3 Schematic illustrations of custom-made prototypes: (a) open cell, (b) closed cell and (c) potentiometric flow cell (13 µL). (d) Potentiometric calibration curve (batch conditions) for nitrate detection for three different membrane compositions. Reproduced with permission from ref. [42]. Copyright 2015,

For nitrite potentiometric sensors, studies have focused on the nitrite selective ionophores rather than the membrane (often the PVC), aiming to prolong the lifetime of the electrodes. Ionophores for NO_2^- were based on the ligand effect to replace the classical "Hofmeister" pattern, relying on membrane doped with anion exchangers (typically the quaternary ammonium ions like tridodecylmethylammonium).[64] According to early research exploiting vitamin B_{12} derivative complexes centered on Co(III), cobalt ion was found to have an axial coordination with NO_2^-, which was selective over chloride[28, 65] due to the formation of σ-π bonds between NO_2^- and Co(III). Since then, Co(III) porphyrins with or without pyridine,[66-69] Co(II) phthalocyanines,[70] analogous Co(III) cobyrinates,[28, 65, 71] and Co(III) corroles[72] were successively introduced as neutral second axial ligand ionophores for nitrite potentiometric sensors. However, because of the response of these ionophores to SCN^-, as well as the cross response from OH^-, it is still difficult to achieve a micromolar sensing range in nitrite potentiometric sensors.[73, 74]

Salen and salophen are another class of ligands capable of binding to a wide range of metals, owing to the Schiff-based properties,[75] which contribute to ion-recognition and enantioselective catalysis.[76, 77] Attempts for nitrite detection have been made with salen and salophen as ionophores,[74, 78-84] and some ISEs had showed impressive selectivity over lipophilic anions.[79, 82] One recent report using a Co(II)/salophen composite in a polymeric membrane reached an LOD below 1 μM level.[85] Besides the performance enhancement and optimization, one of the new research directions with potentiometric sensors is to simultaneously determine various nitrogen ions (including ammonium, nitrate, and nitrite), which is enabled with the help of a 15-ISE electronic tongue system based on a PVC membrane.[86]

2.3 Phosphate detection

In the 1980s, Pungor *et al.* reported a phosphate potentiometric sensor that used phosphate ion-selective electrodes (P-ISEs).[87] However, different from other nutrient ions with a steady molecular structure in solution, as described above, species of phosphate ions are easily transformed among $H_2PO_4^-$, HPO_4^{2-}, and PO_4^{3-} with the variation of pH value (see in Fig. 4a).[88] Therefore, it is difficult to determine each species based on the potential response alone. To date, a variety of P-ISEs have been reported to detect $H_2PO_4^-$, HPO_4^{2-} and PO_4^{3-},[89, 90] and the total phosphate (TP) concentration could be determined with the acidic constants of phosphoric acid (pK_1=2.16, pK_2=7.2, pK_3=12.35) and the pH value of the solution.[91] Except for the pH influence on the mutable formations of phosphates, selective ionophores are needed for phosphate detection since phosphate ionophores are normally sensitive to all three phosphate species.

Phosphate LC-ISEs were applied for detecting phosphate ions based on the exchange of phosphate ions across the solution-phase and the membrane. Organotin was found to be a good ligand for forming complexes with phosphate, and P-ISE was fabricated by a liquid phosphate-sensitive membrane based on dialkyltin(IV) tri-compounds in phosphorus solutions.[92] Later, an LC membrane electrode was replaced by PVC-based polymers with a better mechanical property and stable performance.[93, 94] Polyamine groups modified by macrocyclic,[95] urea,[96, 97] thiourea,[98] and bisthiourea[99] were used as the ionophore, as well as those with central mental cores (*e.g.*, ferrocene,[100] tripodal cadmium complex,[101] and molybdenum[102]) in P-ISEs. Each type of these ionophores have pros and cons based on their sensing performance, *e.g.*, LOD, linear working range, selectivity, and the membrane's lifetime.

P-ISEs with the best LODs were reported with molybdenum acetylacetonate ionophore (1.9 μg L^{-1})[102] and the phenyl urea substituted calix[4]arene immobilized in PVC membrane (0.6 μg L^{-1}).[103] Fig. 4b-c show the structure and sensing response of the phenyl urea substituted calix[4]arene ionophore with an Ag/AgCl reference electrode, which achieved a quick response time of < 8 s. One drawback with this type of membrane is that its performance gradually degraded after 15 weeks, and thus, the long-term stability of phosphate ionophores needs to be improved for practical applications. In addition to direct phosphate sensing, Kaysu *et al.* reported a salicylate-sensitive membrane electrode to detect phosphate indirectly based on the determination of salicylate produced in an enzymatic hydrolysis reaction interfered by the presence of phosphate.[104]

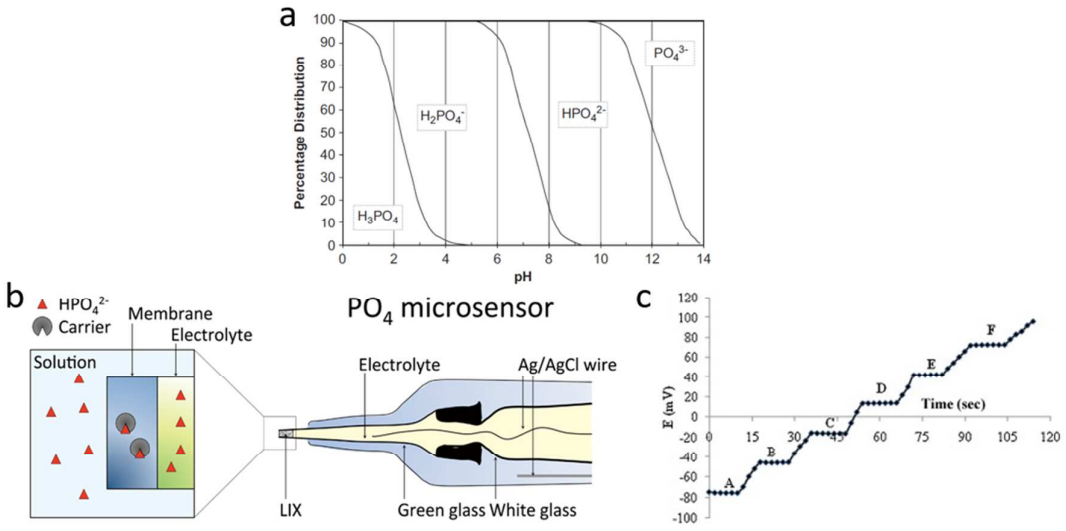

Fig. 4 (a) Distribution of soluble orthophosphate species according to pH at 25 ℃.[88] Reproduced with permission from ref. [88]. Copyright 2013, Elsevier. (b) Scheme of phosphate potentiometric sensor.[105] (c) Dynamic responses (step change) of the electrode in HPO_4^{2-} solution of various concentrations: (A) 1.0×10^{-6} M, (B) 1.0×10^{-5} M, (C) 1.0×10^{-4} M, (D)1.0×10^{-3} M, (E) 1.0×10^{-2} M, (F) 1.0×10^{-1} M. Reproduced with permission from ref. [103] Copyright 2011, Elsevier.

Screen-printed electrodes (SPEs) and carbon paste electrodes (CPEs) were reported for P-ISEs in response to the time-consuming and inconsistent manual fabrication of PVC electrodes.[106-110] Compared with PVC electrodes , CPE has a lower Ohmic resistance and responds to phosphate faster. Moreover, CPE has an easy renewal surface as well as a much longer service life,[111] which is also used in voltammetric sensors.[112, 113] SPEs have been used with commercial printing inks for the potentiometric determination of various species,[109, 114, 115] and they have great potential for the large-scale fabrication of ISEs.

Phosphate SC-ISEs were developed to mitigate the problems with LC-ISEs, *e.g.*, vulnerability to external environment and short lifetime. Cobalt was found potentially responsive to $H_2PO_4^-$ in potassium hydrogen phthalates, and early phosphate SC-ISEs were developed based on cobalt, its alloys, or cobalt oxides. Phosphate sensing with Co-based ISEs is based on the following reactions occurring at different pHs:

$$3CoO + 2H_2PO_4^- + 2H^+ \rightleftharpoons Co_3(PO_4)_2 + 3H_2O \text{ at pH 4.0;} \quad (4)$$

$$3CoO + 2HPO_4^{2-} + 2H_2O \rightleftharpoons Co_3(PO_4)_2 + 4OH^- \text{ at pH 8.0;} \quad (5)$$

$$3CoO + 2PO_4^{3-} + 3H_2O \rightleftharpoons Co_3(PO_4)_2 + 6OH^- \text{ at pH 11.0.} \quad (6)$$

Although the sensors have good responses to phosphates, Co-based ISEs interfered with dissolved oxygen, as well as common anions in water (*e.g.*, HCO_3^-, Cl^-, SO_4^{2-}).[116] This problem was partly overcome by using bis(dibromophenylstannyl)methane as a selective carrier,[105] which exhibited a high selectivity and an LOD of 0.5 µM to HPO_4^{2-}. A potentiometric phosphate biosensor is a special type of phosphate sensor that uses biomaterials, often enzymes, for sensing. Katsu *et al.* applied the alkaline phosphatase to induce the hydrolysis of o-caboxylphenilphosphate, which achieved a detection limit of 0.05 mM,[104] and Menzel *et al.* fabricated a phosphate sensor using a PNP/XOD (endogenous enzymes)/polypyrrole electrode.[5, 117, 118]

With no optimization, the LOD of the potentiometric phosphate sensors was on the order of mg L^{-1} level, which is still high compared with the phosphate concentrations in actual wastewater or eutrophication incept level (as low as 0.01-0.1 mg L^{-1}). Up to now, phosphate ISEs were still being developed without mature commercial product. There is significant room for further development of each component of the P-ISEs, as well as for the optimization of the matrix membrane.

3. Voltammetric sensors

Voltammetric sensors rely on an electrochemical technique for detection, where a potential is applied to drive the chemical reaction (oxidation/reduction) on the electrode/solution interface, which leads to a changed current during detection. Voltammetric sensors are widely used for detecting gases, chemicals, and biomolecules due to their simplicity, portability, low-cost, and high sensitivity.[119-123] Compared with potentiometric sensors, voltammetric sensors have higher sensitivity and can simultaneously detect multiple ions. Many studies have reported the detection of metal ions such as Cd^{2+}, Hg^{2+}, Zn^{2+}, Pb^{2+}, and Cu^{2+} with electrochemical sensors, which also show outstanding performance in detecting nutrient ions such as nitrate, nitrite, and phosphate, among others.

In electrochemical sensors, the catalytic activity of the electrode material determines the sensitivity, specificity, and stability of the sensor. The sensitivity and accuracy of the electrode can decrease due to the poison effect from other species, leading to unsatisfactory performance. Therefore, recent advances aim to develop novel electrode materials, including nanomaterials, biomaterials, and conducting polymers. Since new electrode materials have unique structures and good catalytic

properties, the sensing performance of electrochemical sensors has been rapidly promoted. Moreover, the electrode size, geometry, and surface structure also need attention to meet the requirements for practical applications.

3.1 Device structure and working principle

Voltammetric sensors work by measuring the oxidation/reduction current as the potential of the working electrode is under control. Except for a fixed voltage in amperometry, the ways to apply the voltage includes cyclic voltammetry (CV), square wave voltammetry, and pulse voltammetry. Unlike potentiometric sensors which use dual electrodes, a three-electrode system is employed in the voltammetric sensor (as shown in Fig. 5a). The three-electrode system includes a working electrode (WE) where reduction/oxidation reaction takes place, an RE that ensures the WE potential is accurate, and a counter electrode (CE) which is vital for a complete circuit for ions transfer. Hg/Hg_2Cl_2 and Ag/AgCl electrodes are commonly used as REs, while platinum is adopted in CEs. WE is the key part of the sensor where the electroactive species react. Dropping mercury electrodes, mercury film electrodes, and solid-state electrodes made up of a variety of materials such as precious metals, organic conductive polymers, semiconductors, and carbon-based materials, are widely used. The composition and construction of WE are crucial for the sensor, in which electrode materials with high electrocatalytic activity play vital roles in sensing. The recent development of nanomaterials contributes to the construction of high-performance WE for detecting targets in voltammetric sensors.[124-130] Nanomaterials provide wider and better choices as WE materials due to their large specific surface area, high catalytic activity, and ease of structure modifications.

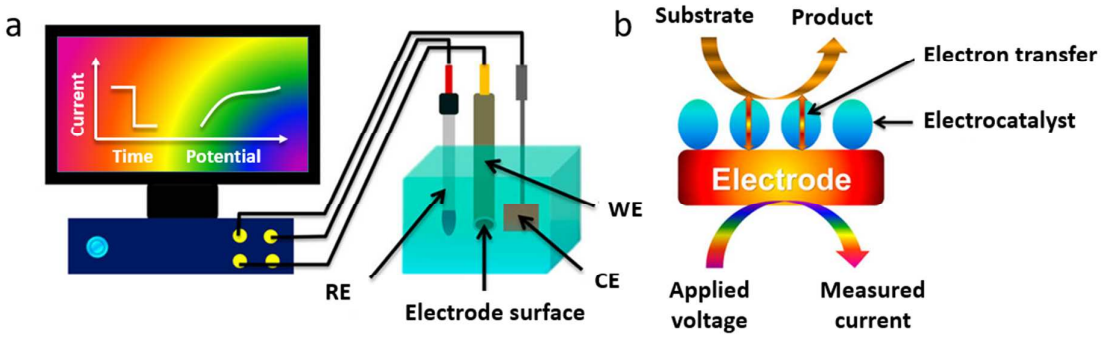

Fig. 5 (a) Structure and (b) working mechanism of a typical voltammetric sensor made up of a reference electrode, a working electrode (WE), and a counter electrode (CE). Reproduced with permission from ref. [131]. Copyright 2016, American Chemical Society.

In a voltammetric sensor, with the force from the external voltage, the sample of interest reacts with working electrode surface based on the electricity-catalysis mechanism, and the dependent variable current is detected as electrical signals that relate to the analyte concentration in the sample. Compared with potentiometric sensors, which have no external power supply but rely on sample concentration difference, voltammetric sensors rely on electricity-driven oxidation/reduction of target species to generate a response signal. Linear sweep CV is a commonly used strategy to determine redox potential and electrochemical reaction rates, whose shape is affected by analyte reduction potential, electrochemical reversibility of electrode reaction, stability of the reduced/oxidized analyte, electrode surface condition, and sweep rate, among others. The working mechanism of the WE is shown in Fig. 5b. The electrode material on the WE surface works as a catalyst to catalyzes the reduction or oxidation of target ion with the help of electricity. The electrode material plays the roles of electrode and catalyst, requiring a high conductivity, a satisfactory activation for substance by decreasing the active energy of reactions, as well as a fairly good chemical stability. The selectivity of sensor relies on the oxidation/reduction potential since different ions are oxidized or reduced at different potentials.

The electrode in the solution under external voltage has excess charge on its surface, which leads to the formation of an electrical double-layer. The sensing is based on electrochemical-dynamic theory. The Nernst Equation was developed to describe the relationship between the electrode potential (E) and the concentrations of species being oxidized or reduced (C_O, C_R) on the electrode surface, and for any of the reversible electrode reaction is written as

$$\mathrm{O} + \mathrm{ne}^- \rightleftharpoons \mathrm{R}. \quad (7)$$

The quantitative relationship can be revealed by the Nernst Equation as:

$$\mathrm{E} = \mathrm{E}^{\theta} + \frac{\mathrm{RT}}{\mathrm{nF}} \ln \frac{\mathrm{C_O}}{\mathrm{C_R}}, \quad (8)$$

where E^{θ} is the standard electrode potential for the reaction, R is the universal gas constant, T is the degree kelvin, n is electron transfer number in molecular redox, and F is the Faraday's constant, respectively. As the sensing signal, the current decides the reaction rates, which is given by the Bulter-Volmer Equation:

$$\mathrm{i} = \mathrm{nFAk}^{\theta}\{\mathrm{C}_0 \exp[-\alpha\eta] - \mathrm{C_R} \exp[(1-\alpha)\eta]\}, \quad (9)$$

where $\eta = \mathrm{nF}(\mathrm{E} - \mathrm{E}^{\theta})/\mathrm{RT}$, k^{θ} is the electrochemical reaction rate, A is the electrode surface area, α is the electron-transfer coefficient. Apart from the electrochemical reaction, the diffusion also influences the electrode process, which is revealed from space (Fick's first law, Eq. 10) and time (Fick's second law, Eq. 11) as:

$$\emptyset = -\mathrm{D}\left(\frac{\partial \mathrm{C}_0}{\partial x}\right), \quad (10)$$

$$\frac{\partial C}{\partial t} = D\frac{\partial^2 C}{\partial x^2}. \quad (11)$$

In Fick's first law, Ø is the diffusion flux, *D* is the diffusion coefficient, *x* is the distance from electrode surface; it describes the relationship between mass transfer and concentration gradient. While the Fick's second law describes the relationship between the concentration gradient and diffusion time.

3.2 Nitrogen salt detection

For nitrogen salt detection, the reports of ammonium voltammetric sensors are very limited because ammonium nitrogen has the most negative valence state (-3) and extraordinary electrochemical stability. Since ammonium is a non-electroactive ion, hardly any electrochemical oxidation take place, even under a much positive potential. Therefore, voltammetric sensors based on the direct oxidation of ammonium are unpractical, and the sensing of ammonium by voltammetry was achieved via indirect methods with the help of transducers.

Enzyme is a typical transducer used in voltammetric ammonium sensors. For instance, enzyme alanine dehydrogenase (AlaDH) has been used in an ammonium working electrode, and the reaction was based on the electrocatalytic oxidation of NADH at the potential of +0.55 V and the sensor achieved an LOD of 0.18 mM.[132] Other enzymes, *e.g.*, glutamate dehydrogenase, have also been employed in NH_4^+ voltammetric sensors in several ways to detect NH_4^+ indirectly. Those enzyme-based NH_4^+ voltammetric sensors have satisfactory selectivity but with a detection limit of mM level.[133-135]

In addition to enzyme, ionophores were also used in voltammetric sensors for NH_4^+ sensing by forming complex, coordination compound, *etc*. In one report, cyclodextrin was used as the ionophore whose association constant is influence by the electrode reaction product, through which the NH_4^+ can be detected from 4.2 to 66 μM.[136] Thiazole benzo-crown ether ethylamine-thioctic acid (TBCEAT) was used to bind with NH_4^+, influencing the redox reaction of the reporter $[Ru(NH_3)_6]^{3+/2+}$ on the Au electrode (Fig. 6a).[137] The sensors were tested by voltammetry (Fig. 6b-e), followed by the selectivity tests over interfering species. The sensor exhibited a good selectivity and a wide linear range from 10^{-6} M to 10^{-1} M of NH_4^+. Other voltammetric sensors for indirect determination of NH_4^+ have also been developed in various designs with a working range from μM to mM.[138, 139]

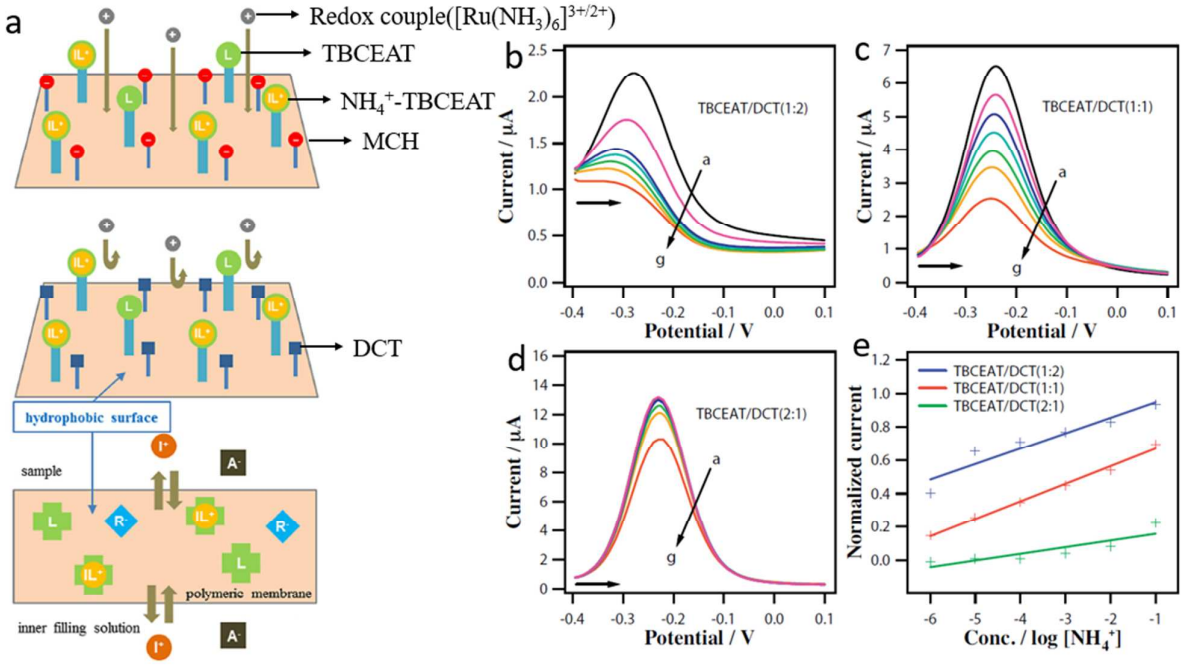

Fig. 6 (a) Schematic diagram of two different types of ion-channel sensing based onthiol-anchored charged (or uncharged) molecules with an uncharged receptor (TBCEAT: thiazole benzo-crown ether ethylamine-thioctic acid, MCH: 6-mercapto hexanol, DCT: 1-decanethiol) and the lower panel shows the conventional ion-selective polymeric membrane for the comparison between ion-channel mimetic sensor (ICS) and ISE. Real square-wave voltammograms of (b) TBCEAT/DCT(1:2)/Au, (c) TBCEAT/DCT(1:1)/Au, and (d) TBCEAT/DCT(2:1)/Au in 0.05 M Tris–H_2SO_4 buffer (pH=7.4) containing 1 mM $Ru(NH_3)_6Cl_3$ with 0.1 M LiCl, and different concentrations of ammonium ion (a→g: 0 M, 10^{-6} M, 10^{-5} M, 10^{-4} M, 10^{-3} M, 10^{-2} M, 10^{-1} M). The scan direction is indicated by a horizontal arrow and the NH_4^+concentration increase by a diagonal arrow. Frequency: 20 s^{-1}. (e) Calibration plots of (b-d) normalized to the corresponding $1-(I_p/I_0)$ (vs. log $[NH_4^+]$), where I_0 is the background peak height, and I_p is the peak height at different concentrations of ammonium ion. Reproduced with permission from ref. [137]. Copyright 2015, Elsevier.

It has been long since the first attempt of the electrochemical reduction of nitrate by Faraday in 1834.[140] The application of voltammetric technique to detect nitrate ions traces back to the 1990s, when electrodes made up of copper were first used to electrochemically reduce the nitrate ion. Various electrode materials were used in nitrate voltammetric sensors,

including metals, alloys, metallic oxide, and carbon materials, as well as their composites.[59, 63, 141] Nitrate can be reduced to nitrite or even ammonium in the electrochemical reaction on an electrode, and this process can be carried out under a rather negative potential of -0.7 V or lower. Side reactions, including anions and oxygen reduction, may occur on the electrode surface,[142, 143] as well as the hydrogen adsorption induced by electrode passivation,[144] which leads to unsatisfactory sensitivity, selectivity, and reproducibility.

Precious and transitional metals are commonly used electrode materials, but copper is the most widely used and exhibits the best electrocatalytic properties for nitrate reduction.[145-150] Nickel (Ni),[151] platinum (Pt),[152] silver (Ag),[153] gold (Au),[154] and cadmium (Cd)[155] have also been employed as electrode materials, but since the bare metal electrodes have shown poor efficiency on electrocatalysis, efforts have been made to promote their performance. Preparing alloys is one of the methods that use the advantages from both metal parts. Cu-Ni,[156] Cu-Cd,[157] and Cu-Pd[158] electrodes were reported with detection limits down to ppm level. Transition metal oxides (TMOs) with enhanced electron transfer property have also been used as the electrode material. For example, zinc oxide (ZnO_2) was modified on Pt as the electrocatalyst, resulting a linear response to NO_3^- from 0.1 to 2.0 mM and an LOD of 10 nM,[159] lower than that of the Zn electrode.[160]

Carbon-based materials are low cost and have good conductivity and chemical stability, and thus they have long been used as electrode materials. In NO_3^- detection, traditional carbon-based materials such as carbon paste (the mixture of graphite powder and a binder pasting liquid) and carbon black were commonly used by means of amperometry.[99, 161] Other carbon-based materials such as boron-doped diamond have also applied.[162] Novel nanocarbon materials such as CNTs and graphene were recently applied as electrode material, showing an enhanced sensing performance due to their nanosize and high electron transport rate.[128, 130, 131, 163, 164]

Apart from CNTs and graphene, other nanomaterials were also adopted for NO_3^- electrodes, such as metals or their oxides with structures of nanoparticle, nanowire, and nanoporous matrix. Nanomaterial-based electrodes have unique dimensions, enhanced mass transport, high effective surface area and, more importantly, excellent electrocatalytic activity (lower negative potential required for electro-reduction). A nanostructured Cu electrode was demonstrated with a 10 μM working range for NO_3^- detection.[165, 166] As shown in Fig. 7a-b, the electrode was made with a vertically aligned Cu nanowire array. The electrochemical detection of NO_3^- was carried out in Na_2SO_4 and H_2SO_4 solution, and the sensor shows a linear working range from 10-400 μM with an LOD down to 1.7 μM (Fig. 7c).[167] On one hand, nanostructures with a large specific surface area provide more reactive sites; on the other hand, they may have an impact on diffusion regime. Another nanostructured electrode based on Cu nanosheets was reported for NO_3^- detection (a linear working range of 1 to 35 μM),[168] superior to that of a microstructured Cu electrode (a linear working range of 10 μM to 1.07 mM).[145]

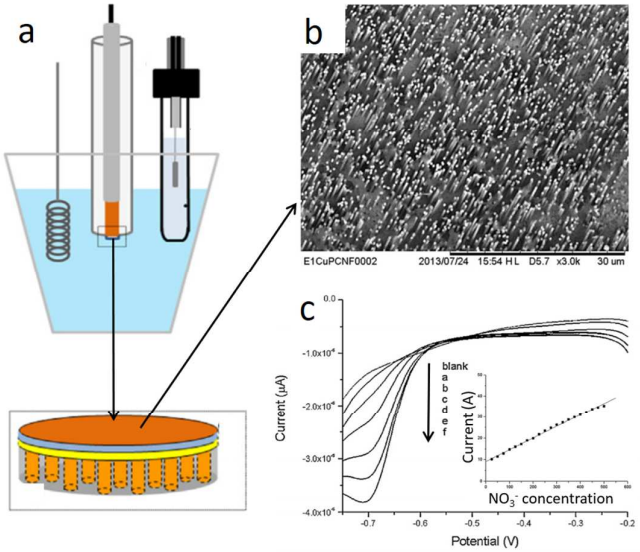

Fig. 7 (a) Scheme of the nitrate sensor and electrode. (b) SEM image of the copper nanowire electrodes (CuWNEEs). (c) Linear sweep voltammetry (LSV) recorded with CuWNEEs in 0.1 M Na_2SO_4, 1 mM H_2SO_4 (scan rate: 0.01 V s^{-1}), at different nitrate concentrations, corresponding to blank, a = 25 μM, b = 100 μM, c = 200 μM, d = 300 μM, e = 400 μM, and f = 500 μM and the calibration plots (inset). Reproduced with permission from ref. [167]. Copyright 2015, Elsevier.

Enzymes (*e.g.*, NaR) are biocatalysts with considerable efficiency and specificity for nitrate reduction, and have been used as the electrode material. To meet the conductivity requirement in WE, reductases are usually combined with other materials that are electroconductive and biocompatible to establish a sufficient electrical communication between the biocatalysts and electrode. Conducting polymers are used as matrix to immobilize the enzymes. For instance, viologen acrylamide copolymer, polythiophene-bipyridinium polymer, and amphiphilic polypyrrole monomer (viologen) were used and performed as mediators for

nitrate reduction by transforming the oxidation and reduction state. In addition, their sensing performance was no worse than inorganic materials with an LOD down to 10 μM or even lower.[61, 169-172]

Structure modifications of the electrode material can improve catalyst performance and extend the sensor dynamic range. One of the major concerns for all electrochemical nitrate sensors is the nonspecific adsorption of coexisting species, especially heavy mental ions on the electrode surface. To solve this problem, chitosan was used as a permselective membrane due to its high diffusional resistance for interferents and low diffusional resistance for the analytes.[159] Activating the electrode surface, *e.g.*, Cu[165] and Cu microelectrode arrays,[145] is another method to enhance electrode performance, in which chloride ions are added to obtain an activated catalyst surface. As a result, the electrode exhibits better sensing performance on sensitivity and stability.

Voltammetric determinations for nitrite were widely studied and reported. Nitrite is electroactive on variety of materials such as glassy carbon (GC), Cu, Ni, Pt, Au, diamond, alloys, and TMOs.[173-176] Because of the intermediate valence of nitrogen in nitrite (+3), the electrochemical determination is based on either reduction or oxidation, which depend on the electrode potential. However, detection based on reduction exhibited poor sensitivity and selectivity[177] due to the interference from oxygen and nitrate ions. Therefore, detection with an oxidation process with a product of nitrate was often adopted.[178] To oxidize nitrite at an unmodified electrode, a large overpotential is required as well as poor electron-transfer and electrode passivation,[179] which is the main focus of research on electrode materials.[180]

A variety of metals and intermetallic compounds have been employed in NO_2^- sensors, and most of them have been used in NO_3^- and NO_2^- sensors with distinct applied potentials (negative in the former and positive mostly in the latter). Among these materials, Indium tin oxide (ITO) was used as the sensor electrode and exhibited outstanding performance, but its high-cost and poor stability hamper its application.[181] Carbon materials with a better chemical stability and conductivity were used in sensor electrodes and are electroactive due to the defects in their microstructures. Carbon paste electrodes[182] have been used both on nitrate and nitrite voltammetric sensors, with LODs of 87 mM for nitrate and 0.625 μM for nitrite, respectively.[10] Although diamond has been used as the catalyst on the electrode, it is expensive and unsuitable for manufacturing, and thus hinders practical application.[15] C_{60} has been fabricated in a working electrode with a fairly good sensitivity and stability.[128] CNT and graphene-based materials also have been widely studied as electrode materials in recent years. Besides the general advantages of nanomaterials such as high specific area with more active sites, they have showed excellent adsorption for analysts, as well as outstanding electroconductivity and electrochemical stability, which contribute to the easier oxidation of nitrite on an electrode.

In addition to NO_3^- sensors, nanomaterials also offer unique properties and high performance in voltammetric NO_2^- sensors. Nanostructured metals are commonly used as a catalyst on an electrode and have been combined with a wide variety of materials to form composite electrode materials.[183-185] With CNT as the substrate, a variety of materials were employed in composite electrodes, including metallic nanoparticles like Cu,[186] Au,[187] Ag,[185] Pd,[183] Pt[188], metal oxides like PdO,[181] nanostructured carbon black,[161] and nano-organics such as carboxylated nanocrystalline cellulose.[189] As show in Fig. 8a-c, three electrodes were prepared by pristine single-walled CNT (SWCNT) film and spherical and urchin-like Pd NPs patterned SWCNT film. The electrochemical test results shown in Fig. 8d-e revealed the enhanced electroanalytic property of the electrode with Pd NPs, especially the urchin-like Pd NP. The sensing performance of the Pd/SWCNT is shown in Fig. 8f-g; the LOD of this sensor was determined to be 0.25 μM.[183] The superior sensing performance of urchin-like Pd NPs over spherical Pd NPs was attributed to the different catalytic property of the Pd nanostructure facets exposing to analytes. Since anisotropic nanoparticles were found to have extraordinary electrochemical activity compared with isotropic ones,[190-192] attempts have been made to apply anisotropic nanoparticles in electro-analysis for many substances and enhanced sensing performance.[193-196] Graphene, the representative two-dimension (2D) nanomaterial, has been used in composite electrodes similar to that of CNT.[184, 197-199] For example, metallic nanoparticles (Au and Co NPs)[185, 200, 201] and metal oxide NPs (Cu_2O, TiO_2, and ZrO_2),[202-204] were deposited on the surface of graphene for detecting NO_2^-. Other nanomaterials have also been reported with fairly good performance in NO_2^- sensors. Fe_2O_3 NPs – coated ZnO nanorods grown on a silver electrode achieved a linear response to NO_2^- from 1 to 1,250 μM with a high sensitivity of 131.2 μA μM^{-1} cm^{-2}.[176] SiC NPs immobilized on a glassy carbon electrode via ionic liquid have a linear working range from 50 nM to 350 μM, with an LOD as lower as 20 nM.[205] Nanocomposites like polyaniline/Cu[206] and graphite oxide/Pd[184] were also reported as electrode materials in NO_2^- sensors.

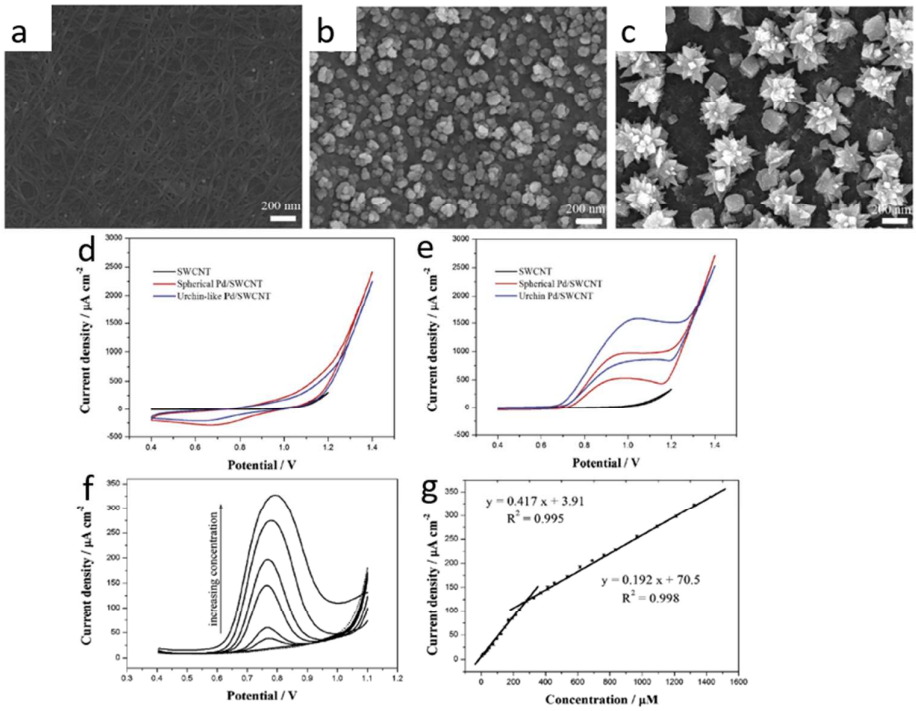

Fig. 8 SEM images of (a) pristine SWCNT film and (b) spherical Pd NPs and (c) urchin-like Pd NPs patterned SWCNT film electrodes. Cyclic voltammograms of pristine SWCNT thin film and Pd/SWCNT film electrodes (d) in the absence and (e) presence of 2 mM nitrite in PBS (pH 7.0) at a scan rate of 50 mV s^{-1}. (f) Differential pulse voltammograms. Nitrite concentration: 0, 10, 48, 91, 304, 500, 880, and 1231 μM in deoxygenated PBS (pH 4.0) solution (from bottom to top). (g) Calibration plots. Reproduced with permission from ref. [183]. Copyright 2014, Elsevier.

Enzymes with a special molecular recognition show high selectivity in NO_2^- detection. Different from other nitrite voltammetric sensors via catalytical oxidation, enzyme electrodes are based on the reduction of nitrite with nitrite reductases (NiRs). However, since enzyme is non-conductive, conductive mediators and matrix were employed together with enzymes on the electrode. For example, copper-containing NiR (Cu-NiR) was immobilized in viologen-modified chitosan on a glassy carbon electrode (CHIT-V); the working mechanism is shown in Fig. 9. The redox-active viologen acts as a mediator that directly reacts on the electrode surface, providing electrons for Cu-NiR to reduce the NO_2^- ions, while chitosan-immobilized viologen and the Cu-NiR achieve effective electron transport from viologen to Cu-NiR.[207]

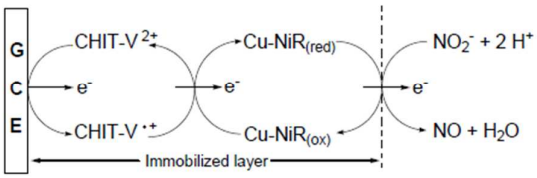

Fig. 9 Scheme of working principle of the co-immobilized Cu-NiR and CHIT-V GCE. Reproduced with permission from ref. [207]. Copyright 2014, Multidisciplinary Digital Publishing Institute.

Structure designs of the electrode material provide more choices and possibilities for high-performance sensors, including surface modifications, doping, introducing polymers, and compositing with 1D/2D nanostructured substances. Polymers have been extensively used as the matrix to immobilize the catalysts or ion recognizer, and in some conditions, as the electron transducer. As one of the most widely used natural polymers, chitosan has been employed with metal nanoparticles,[10] carbon nanomaterials,[186, 200] and enzymes,[207, 208] among others. An example of chemically modified chitosan variants in an NO_2^- sensor exhibited good stability, with a linear response up to 11 μM and an LOD of 40 nM.[207]

3.3 Phosphate detection

Phosphate ions are not directly accessible to voltammetric sensors since phosphate reduction/oxidation is largely inhibited by oxygen ions around the central phosphorous atom. As a consequence, voltammetric detection of phosphates almost relies on indirect solutions. Because of the different approaches adopted for phosphate detection, the constructions and materials used on the electrode thus are different from those used for nitrate or nitrite sensors.

One of the designs for phosphate voltammetric sensors is based on the receptor for phosphate, which can attract phosphate ions, and has an impact on a certain redox reaction called the host-guest interaction. For example, bisthiourea was used as the receptor, as its attraction for orthophosphate inhibited the redox reaction of an electron transfer (potassium hexacyanoferrate). Thus, phosphate ions could be determined indirectly with a high selectivity over SO_4^{2-}, NO_3^-, Cl^-, and a detection limit of 16 mg L^{-1}

(0.17 mM) for $H_2PO_4^-$.[209] In the same way, $H_2PO_4^-$ was detected by using bisacrylamide cobaltocenium, which has a high affinity for $H_2PO_4^-$.[210] The sensor could detect $H_2PO_4^-$ with a concentration of 31 mg L^{-1}, and its sensitivity was much higher than Cl^- (2.7 times higher) and Br^- (7.0 times higher). Other indirect voltammetric sensors that used biomaterials, which directly detect other species, have also been employed to determine phosphates. For example, the H_2O_2 sensors based on screen-printed carbon responded to H_2O_2, which was produced from the electrocatalytic reaction in the presence of phosphates, oxygen, and cofactors, achieving a linear detection range from 22.7 µM to 181 µM and an LOD of 4.27 µM.[211]

Stefano *et al.* reported a paper-based electrochemical phosphate sensor manufactured with a simple and inexpensive approach (Fig. 10a-b).[212] The detection of phosphate was achieved by using ferricyanide as the redox mediator. The electrochemical sensing results, shown in Fig. 10c-d, indicate that carbon black could enhance the sensitivity and the ferricyanide is critical in the sensing process. The LOD of the sensor is 4 mM with a wide linear range up to 300 mM. Electrochemical sensors detected phosphates ions by quantifying the anodic oxidation of molybdenum[213] or reducing the phosphomolybdate complex[214, 215] have also been reported. These indirect voltammetric methods usually require reagents and have a working range between 0.02 to 1 mg L^{-1}. Since phosphate and ferrocene derivative have a competitive effect with each other when attracting onto the cavity of a cyclodextrin derivative, phosphate has also been indirectly detected by using cyclic oligosaccharide (β-amino-cyclodextrin) with ferrocene derivatives in solution.[93] In this sensor, cyclodextrins on Au electrode responded to ferrocene and the reaction was affected by phosphates.[216]

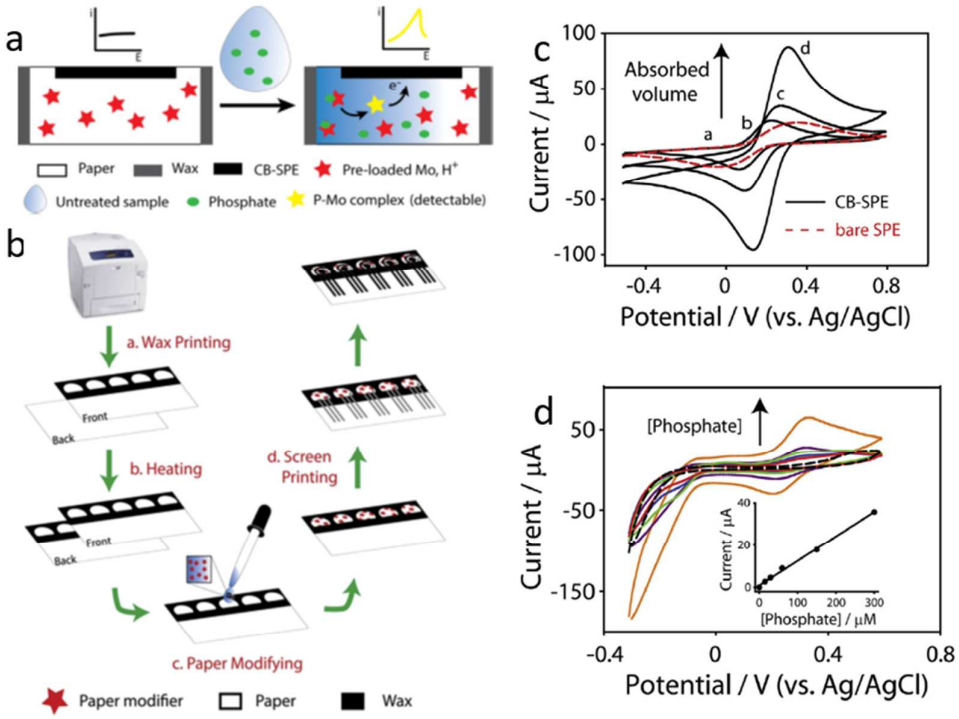

Fig. 10 (a) Scheme of the structure, working principle and (b) fabrication steps to produce reagent-free paper-based electrochemical sensors. (c) Cyclic voltammetric results of graphite-based ink-printed paper modified with 5 mL of 10 mM ferricyanide (a.) and CB-based ink printed onto paper modified with 5 mL (b.), 10 mL (c.), and 20 mL (d.) of 10 mM ferricyanide. Scan rate: 100 mV s^{-1}. (d) Voltammograms obtained for different phosphate concentrations, from 0 to 300 mM, obtained using CB-based ink printed onto paper modified with 10 mL solution containing 100 mM molybdate, 100 mM potassium chloride and 100 mM sulfuric acid. Reproduced with permission from ref. [212]. Copyright 2016, Elsevier.

The use of enzyme electrodes for detecting phosphate has achieved high selectivity because of their specific molecular bio-recognition.[4, 17, 217] Electrochemical biosensors for phosphate are based on either the production of H_2O_2 byproduct or the consumption of molecular oxygen. Typically, one or more enzymes, such as pyruvate oxidase (POD) or alkaline phosphatase (AP) were immobilized onto an electrode and then the product from catalyzed reaction or the reactants was detected by voltammetry.[11, 17] The sensors work based on the determination of dissolved oxygen with the help of pyruvate oxidase and the detection of hydrogen peroxide with the use of nucleoside phosphatase or xanthine oxidase. However, these voltammetric biosensors based on enzymes have an uncertain stability and doubtful durability, and are expensive due to the high cost of enzyme.[218] An alternative strategy exploited the affinity between phosphates and enzyme electrode, which was used to detect glucose whose concentration is influenced by presence of phosphate ions. The response of glucose could indirectly detect phosphate with a linear response from 1.2 to 31 mg L^{-1}, an LOD of 9 µg L^{-1}, and a good selectivity.[219]

Non-biotic materials are preferred to enzyme electrodes in terms of the low-cost and high chemical stability. For example, β-amino-cyclodextrin was used as an enzyme-free electrode in voltammetric phosphate detection based on its affinity to phosphate ions.[220] Pt and Au microelectrode arrays modified by pyrrole-ferrocene derivative were prepared to selectively detect phosphate ions with an LOD of 1.04×10^{-6} M.[221] Molecularly imprinted polymers (MIPs) were recently developed as a specific molecular recognizer for selective detection of phosphates, in which a phosphate MIP from methacrylic acid and N-allylthiourea was reported for phosphate detection,[222] suggesting MIP has a high potential as an electrode material for specific phosphate sensing.

4. Field-effect transistor (FET) sensors

4.1 Device structure and working principle

For detecting various hazardous chemicals and environmental pollutants, FET-based sensors are rising as a powerful sensing platform, attributing to their outstanding performance, *i.e.*, ultrahigh sensitivity, easy operation, and near real-time response compared with conventional techniques (*e.g.*, chromatography, mass spectrometry).[223-225] As shown in Fig. 11, generally, an FET device consists of source, drain, and gate terminals, a gate insulator layer, and a semiconducting channel for the sensing. Most FETs also have a fourth terminal called the body, base, bulk, or substrate, which serves to bias the transistor into operation. The platform works by monitoring the conductivity difference between the drain and source terminals, which is controlled by an electric field in the device. The electric field is generated by the voltage difference between the body and the gate of the device, and it varies accordingly when the sensor is exposed to different concentrations of target solutions.

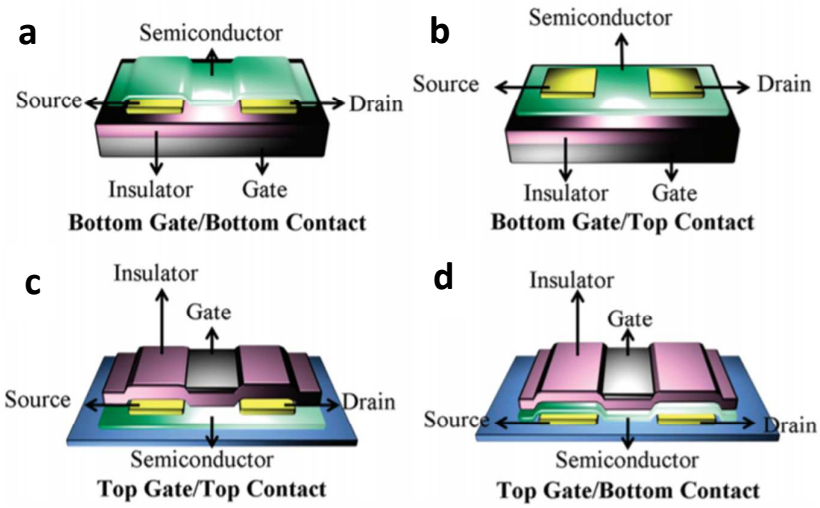

Fig. 11 Four types of FET device structures: (a) bottom gate/bottom contact; (b) bottom gate/top contact; (c) top gate/top contact; and (d) top gate/bottom contact. Reproduced with permission from ref. [226]. Copyright 2012, American Chemical Society.

An ion-selective field-effect transistor (ISFET) is a sensing platform that integrates an ion-selective membrane with an FET device. The working principle of an ISFET is based on the change of gate potential on the sensing channel through the accumulation/adsorption of target ions. In the ISFET, normally the input works through the metal top gates, *e.g.*, ISFET pH electrode. Other ISFETs consist of a gate insulator (Si_3N_4) and metal gate oxide (SiO_2),[227, 228] as shown in Fig. 12a. When the ion concentration (such as H^+) changes, it changes the gate potential and thus the current through the transistor will change accordingly. Compared with the ISE, ISFET was constructed into one device in which the sensing surface and a single amplifier deliver a high current signal and no internal solution is needed. It provides ISFET with many advantages, including quick response, smaller size, low output impedance, and the ability for mass fabrication with a low cost.[229, 230]

The chemical sensitivity of the pH-sensitive gate of an ISFET can be altered if a membrane is deposited onto the gate insulator, thereby developing a chemically-modified FET (ChemFET).[231] In Fig. 12b, pH-buffered hydrogel was attached covalently to the gate oxide of the FET device, followed by the plasticized PVC membrane attached to the top. Various membranes from conventional ISEs,[232] which can selectively detect ion activities, have been applied in ChemFETs to improve the selectivity of the sensor.[231] Ion-selective ChemFET sensors were reported with a nitrate-selective membrane based on photocurable material,[233] an ammonium membrane based on self-plasticizing material,[234] and a phosphate membrane with PVC containing lipophilic uranyl salophene derivatives.[235] In principle, the ChemFET response lies in the complexation of the analyte with the ion carrier at the outer phase boundary,[227] which will generate potential difference at the interface of membrane/aqueous solution, and thus result in the conductivity change of the semiconducting channel material.[236] The response times of ChemFETs are on the order of a few hundred milliseconds, which enables real-time detection of target ions.

Many studies have reported FET sensors using various functionalized nanomaterials, which work as the sensing channel and bring tremendous opportunities in the low-level detection of water contaminants, *e.g.*, heavy metal ions, nutrients, and bacteria.[223-225, 237-240] The basic mechanism of the sensor is the adsorbate-induced perturbation-induced conductance change in the channel material, typically, in terms of the source-drain current of the FET device. Since the intensity of conductivity change usually depends on the target ion concentration, the FET sensor could quantitatively measure ions in water. For selective detection of the target ions, the channel material is usually functionalized with specific probes. Channel material with a high surface-to-volume ratio is favored, since it leads to a high adsorption site density.[225] Consequently, 2D semiconducting materials are promising candidates for sensing applications. In the last decade, various nanomaterials have been employed as channel material for FET sensors, including nanorods,[241, 242] nanowires,[243-245] CNTs,[246-248] graphene,[223, 225, 249] black phosphorene,[250, 251] and molybdenum disulfide nanosheets.[236, 237] Due to their unique structures and properties, *e.g.*, high sensitivity to electronic perturbations of nanomaterials, nanomaterial-based FET sensors usually exhibit high sensitivity, low detection limit, and rapid response to water contaminants. These unique features enable the rapid detection of water contaminants and address limitations of conventional sensing technologies. This section focuses on FET sensors, which use 1D or 2D semiconducting nanomaterials as the sensing channel, for detecting nutrients.

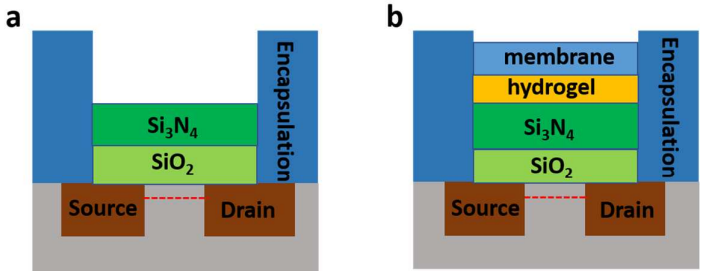

Fig. 12 Cross-section views of (a) ISFET and (b) ChemFET.

4.2 Nitrogen salt detection

Most nitrate-sensitive FETs (NO_3^- ISFET) have been fabricated on a p-type substrate with an SiO_2 and Si_3N_4 layer. The gate terminal was prepared with electroactive material by functionalizing the grafted chlorosilane with trimethylamine, or with trioctadecylmethylammonium nitrate (TODMA). The detection limit varies from μM to mM, a response time of seconds; a lifetime from weeks to several months, and a selectivity from NO_2^-, Br^-, I^-, Cl^-, $H_2PO_4^-$, and SO_4^{2-}.[252-254] Polysiloxane copolymer membrane was used for the nitrate-selective ChemFET,[255] with the detection limit of $1\times10^{-3.9}$ M and improved durability over 190 days. Wróblewski *et al.* optimized the nitrate detector using the ChemFET based on an o-NPOE/PVC membrane containing 1% of symmetrical tetradodecylammonium nitrate (TDDAN), which showed a good selectivity and improved durability for at least three months with an LOD down to 10^{-6} M.[256] Other researchers also reported the membrane using a TDDAN ligand, which showed superior selectivity for the nitrate ion.[257]

Besides using traditional Si-based FET for detecting NO_3^-, other FET sensors based on materials with high electron mobility have be developed, *e.g.*, AlGaN/GaN. Myers *et al.* demonstrated a FET nitrate sensor with an AlGaN/GaN heterostructure functionalized with ion-selective membranes.[258] Different from Si-based transistors, the AlGaN/GaN-based transistors do not require a gate bias to be turned on; therefore, no gate electrode is required when it is used as an ion-sensing transistor device. A plasticized PVC-based membrane was formed in-situ by dropping the nitrate selective ionophore solution directly onto the gate region. The sensor showed a good performance with a fast response, an LOD of $1\text{x}10^{-7}$ M (6.2 ppb), and a wide detection range of $1\text{x}10^{-6}$ – $1\text{x}10^{-2}$ M (62 ppb – 620 ppm).

Integrated enzyme-functionalized FET (ENFET) was demonstrated for sensing nitrate.[259] The detection was based on the affinity binding of the enzyme to an electron-relay, which mediated the electron transfer to the enzyme and simulated the reduction of nitrate. The gate interface was modified with *N*-methyl-*N*A-(carboxyalkyl)-4,4A-bipyridinium relay units, and a stable relay-enzyme layer on the gate surface was generated through the crosslink between the nitrate reductase and the bipyridinium units with glutaric dialdehyde. The nitrate reductase (sodium dithionite) was used as the electron donor to simulate the reduction of nitrate to nitrite. The concentration of NO_3^- ions in the system regulated the ratio of oxidized/reduced states of the relay, thereby controlling the gate potential. The ENFET device-based nitrate sensor responded in less than 50s, had an LOD of 7×10^{-5} M for nitrate, and a sensitivity of 52±2 mV dec^{-1}.

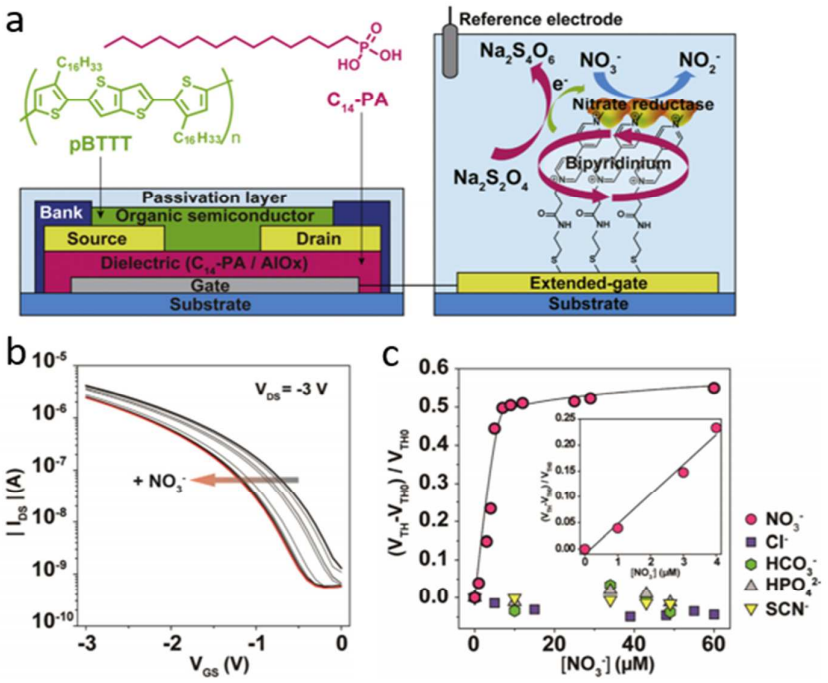

Fig. 13 (a) Schematic illustration of the nitrate sensing device based on extended-gate type. (b) Transfer characteristics (I_{DS}-V_{GS}) of the OFET sensor upon titration with nitrate in a HEPES buffer solution (10 mM) with $Na_2S_2O_4$ (20 mM) at pH 7.4. V_{DS}= –3.0 V. [Nitrate] = 0–60 mM. (c) Changes in the threshold voltage (V_{TH}) of the OFET device by adding a NO_3^- solution with various concentrations in a HEPES-buffer solution (10 mM) with $Na_2S_2O_4$ (20 mM) at pH 7.4. Inset shows the lower end of the nitrate titration. Reproduced with permission from ref. [260]. Copyright 2016, Elsevier.

FET sensors using organic semiconductors also get numerous attention attribute to their intriguing properties, such as stretchability, mechanical flexibility, printability, and low fabrication cost. Minami *et al.* reported the first selective nitrate sensor based on an extended-gate type organic field-effect transistor (OFET).[260] As shown in Fig. 13a, the sensor consists of an OFET-based transducer and an extended-gate electrode functionalized by a nitrate reductase with a mediator (=bipyridinium derivative/BP). The solution-processable PBTTT (poly 2,5-bis(3-hex-adecylthiophene-2-yl)thieno[3,2-b]thiophene) was used as the organic semiconductor in the OFET. The nitrate detection mechanism can be explained by an electron-relay on the extended-gate electrode. The addition of nitrate enables the enzyme reaction ($BP^{2+} \leftrightarrow BP^{+}$), which leads to the change of the electron mediator (=BP) valence. This results in the potential change in the gate electrode, which reflects as the shifting of V_{th}, as shown in Fig. 13b. In this report, 90% of the sensors responded in within 20s with a linear working range of 0–4.0×10^{-6} M. The LOD of the nitrate sensor in water was estimated to be 45 ppb, which is lower than or comparable with those of the in-organic FET-based sensors and some conventional detection methods. The highly selective response to nitrate was confirmed by testing some representative small anions, *e.g.*, Cl^-, SCN^-, HPO_4^{2-}, HCO_3^- (Fig. 13c). Nitrate detection in diluted human saliva has also been demonstrated, implying the potential of practical applications of the OFET sensor.

To the best of our knowledge, there are not many nitrite-selective FET sensors reported in the literature. Antonisse *et al.* reported that polysiloxanes with different types of polar substituents (acetylphenoxypropyl or phenylsulfonylpropyl) are excellent membrane materials for nitrite selective ChemFET by incorporating cobalt porphyrin.[261] The nitrite selective ChemFET showed a response in the concentration range 1×10^{-3}–0.1 M and a high selectivity over chloride and bromide. An LOD of 2×10^{-4} M was obtained in the presence of 0.1 M bromide. Wróblewski *et al.* presented an NO_2^--selective FET device based on a PVC-plasticized membrane, which used a uranyl salophen derivative as the anion-sensitive receptor.[81] The designed sensor showed a linear response in the range 10^{-4}–10^{-1} M with a good selectivity for nitrite ions over other inorganic anions.

For detecting ammonium, metal oxide semiconductor FET (MOSFET) sensors have been reported.[262] In these sensors, NA is a commonly used neutral carrier in the plasticized PVC membrane. ISFET using a membrane containing synthetic neutral carrier ETH 227 and NA was designed to test ammonia, which showed a quick response of 15 ms.[263] The sensor exhibited an LOD around 6×10^{-4} M, with a lifetime of approximately 20 days. Kazanskaya and others demonstrated an ammonia FET sensor with a robust polymer photo- and ion-sensitive membrane, which was fabricated from polyethylene terephthalate (PETPh) film modified with spiropyran (SP) and NA.[264] The membrane generated photopotential upon UV irradiation, which related to the NH_4^+ concentration in solution. The optimal sensor exhibited a working range of 10^{-6}–10^{-4} M for NH_4^+. Detection was also conducted with a urea sample, which showed a sensing range of 10^{-5}–10^{-3} M with immobilized urease as a catalyst. Another application of NA in a plasticized PVC

membrane, fabricated by integrating both ammonium and reference (non-sensitive) FET, was used for the ammonium sensing.[265] By measuring the differential between both FETs, the system reduced the interference from the Na^+ and K^+ ions and the effect of ionic strength and temperature, and showed an LOD of 2×10^{-6} M. An AlGaN/GaN-based ChemFET sensor also was fabricated to detect NH_4^+. The sensor consists of a high-electron-mobility transistor device with a non-metallized gate, coated with NA-modified PVC membrane.[231] The AlGaN/GaN NH_4^+ sensor obtained a constant sensitivity for various NH_4^+ concentrations ranging from 10^{-5} to 10^{-2} M, with an LOD of 5.4×10^{-6} M, which is approximately one order of magnitude lower than those with Si-based ChemFETs.

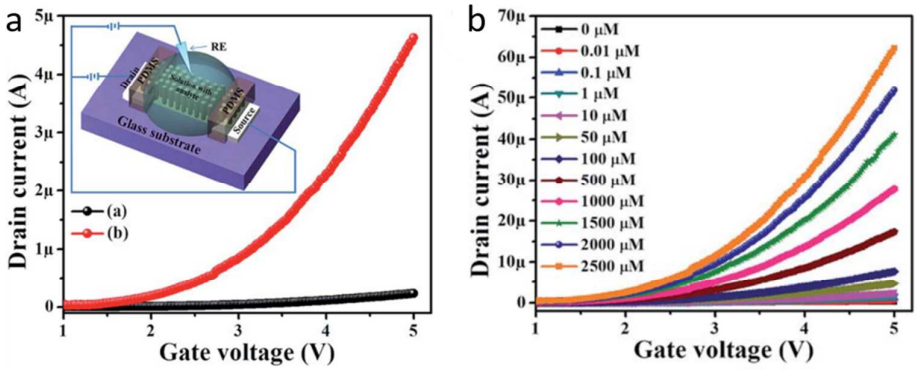

Fig. 14 (a) I–V response of an FET-based ammonium sensor without (black) and with (red) 50 mM ammonium ion in 0.1 M PBS solution (pH =7.0). Inset schematically shows the experimental setup. (b) I–V response of the sensor with increasing concentration of ammonium in 0.1 M PBS solution (pH= 7.0) at a fixed gate–source voltage range of 1.0–5.0 V through an Ag/AgCl reference electrode. Reproduced with permission from ref. [241]. Copyright 2016, Royal Society of Chemistry.

Semiconducting nanomaterials, *e.g.*, nanorods, were also investigated as promising sensing channel materials in NH_4^+ MOSFET sensors. ZnO has been widely studied in FET devices due to its wide band gap (~3.37 eV) and high exciton binding energy (60 meV). A ZnO nanorod-based FET device was reported by Ahmad *et al.* for detecting ammonium.[241] The sensor was fabricated with vertically aligned ZnO nanorods by growing the nanorods directly on the seeded glass substrate between the pre-deposited source and drain electrodes. The drain-source current vs. gate potential was used as the electrical sensing signal of the sensor (Fig. 14a). The surface of ZnO nanorods is sensitive to both oxidizing and reducing analytes, attributing to the presence of adsorbed oxygen on the outer layer, which is ionized into different oxygen species. In principle, the reaction between the active surface-adsorbed oxygen (O_{ads}^-) and the NH_4^+ released the trapped electrons to the conduction band of ZnO nanorod, which increased the conductivity of the ZnO nanorod. As shown in Fig. 14a, the sensor current greatly increased in the presence of NH_4^+, which was related to the concentration of NH_4^+ (Fig. 14b). The fabricated FET sensor showed excellent sensing performance with rapid response, an LOD of 0.07 μM, a linear range from 0.07 μM to 1 mM, and stable performance for 10 weeks. The direct synthesis of ZnO nanorods on an active area provides high surface area and easy substrate penetration structures, which improves the reproducibility and stability for detecting NH_4^+ in solution.

4.3 Phosphate detection

Phosphate ChemFETs used non-redox active host (*e.g.*, cationic polymer) to extract phosphate ions into an inert membrane (*e.g.*, PVC membrane). Liu *et al.* designed an FET $H_2PO_4^-$ sensor based on the ion-selective coated-wire/FET electrode.[266] In the phosphate FET, they used cobalt phthalocyanine as ion-exchange electroactive substance and PVC as the membrane matrix, which was coated on a platinum wire. The wire was connected to the FET and the drain current change depended on the phosphate concentration. This HPO_4^{2-} FET sensor exhibited a linear response in the range of 10^{-5}-10^{-1} M, with high selectivity and a response time around one minute. The limiting factor of this FET is the presence of chloride generated interference, and thus the sensing electrode must be replaced every month. Antonisse *et al.* reported a sensor using a plasticized PVC membrane containing 1% uranyl salophene derivatives as the membrane matrix, which showed a high selectivity of phosphate over much more lipophilic anions, *e.g.*, nitrate.[235]

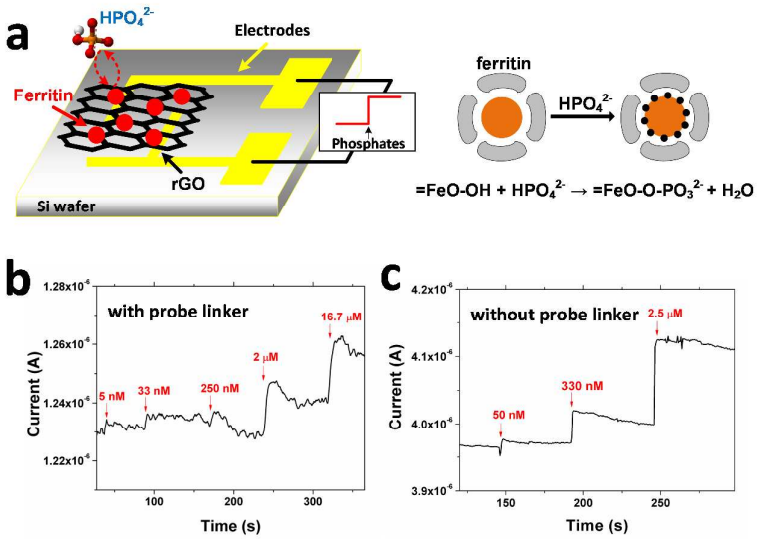

Fig. 15 (a) schematic of the rGO/ferritin sensing platform for HPO_4^{2-} detection. (b) and (c) Dynamic responses of the rGO/ferritin sensors to HPO_4^{2-} of different concentrations with and without the probe linker. Reproduced with permission from ref. [267]. Copyright 2017, Royal Society of Chemistry.

Graphene and reduced-graphene oxide (rGO) have been employed as the channel material in FET sensors due to their unique 2D structure and outstanding properties.[225, 268-274] Graphene has a high electrical conductivity (3,189 S cm^{-1}),[275, 276] an ultrahigh electron mobility (200,000 cm^2 V^{-1} s^{-1}),[277] and an extremely high surface-to-volume ratio (2,600 m^2 g^{-1}). Moreover, graphene has exceptionally low electronic noise, which enables the sensitive detection of various analytes.[278] Mao *et al.* reported the detection of orthophosphate ions (HPO_4^{2-}) with an FET sensor based on rGO/ferritin,[267] as shown in Fig. 15a. The detection is realized by monitoring the orthophosphate ions-induced conductance change on the sensing material (rGO) between the source and drain electrodes. The sensing surface was functionalized with ferritin, which formed a hydrated iron oxide mineral core and acted as sorbent for orthophosphate ions. The adsorption of HPO_4^{2-} caused the current increase in the channel (as shown in Fig. 15b-c). The sensor showed an LOD of 26 nM (phosphorus concentration: 0.8 μg L^{-1}) and a response time on the order of seconds. The FET also exhibited a good selectivity over Cl^-, SO_4^{2-}, and CO_3^{2-} ions. The sensitive, selective, and quick response implies a promising application of FET sensors in detecting phosphorus and thus offers a new sensing platform for the low concentration and real-time monitoring of nutrients in water.

FET sensors based on pyruvate oxidase (PyO)-functionalized ZnO nanorods (ZnO NRs) array was also reported for phosphate detection.[242] The ZnO NRs array was directly grown on seeded SiO_2/Si substrate via a low-temperature aqueous route. This method provided the ZnO nanorods with a high surface area for enhanced PyO immobilization and thus improved the specificity for phosphate detection. The detection relied on the fact that the PyO adsorbed on the ZnO NRs surface catalyzed the reaction of pyruvate and phosphate ion (Eq. 12), which generated H_2O_2 and acetylphosphate:

$$\text{Pyruvate} + \text{Phosphate} + O_2 \rightarrow \text{Acetylphosphate} + H_2O_2 + CO_2. \quad (12)$$

The fabricated FET sensor is highly sensitive to phosphate ion, demonstrating 80.57 μA mM^{-1} cm^{-2}, with a wide linear range from 0.1 μM – 7.0 mM. The PyO-functionalized sensing platform also showed very low responses to interfering species (K^+, SO_4^{2+}, Ca^{2+}, HCO_3^-, and thiamine pyrophosphate chloride) at 0.1 mM.

Currently, there are very few reports of FET sensors used for nutrient monitoring. However, since FET sensors have shown outstanding performance in detecting gas and biomolecules with very high sensitivity and real-time response, they have a great promise in detecting water contaminants. Moreover, with the development of novel 2D semiconducting nanomaterials and their nanocomposites, it is envisioned that the performance of the FET sensor would be further enhanced to meet the requirements for real applications in water quality monitoring.

5. Conclusions and outlook

In this review article, representative potentiometric, voltammetric and FET sensors for detecting nutrients have been introduced. Compared with conventional sensing methods, which are time-consuming, expensive, and need specially trained personnel to operate, interest in electronic sensors is rising due to their outstanding performance, *i.e.*, high sensitivity, easy operation, fast response, miniaturized size, and low manufacturing cost, making them an intriguing sensing platform. Table 1 summaries representative electronic sensors and their sensing performance for nitrate, nitrite, ammonium, and phosphate detection in an aqueous environment. With novel sensing elements or structures (*e.g.*, composite membranes, nanomaterials, enzymes), some of the sensors show good LOD and selectivity with a rapid response feature; however, most of the sensors still suffer from limitations such as interference from other ions, low selectivity, unstable performance, and poor reproducibility. Although great progress has been made to address these limitations, tremendous work is still needed for real applications and commercialization of electronic sensors.

For potentiometric sensors, major concerns for their real applications are selectivity and interference from other ions. For ion-selective electrodes, various chemicals have been used as a modifier to extract target ions into the membrane matrix, and thus the quantification test. However, since the selectivity depends on the ISE, ions with similar structures and properties may lead to challenges with selective detection. Also, the diffusion of ions may be impacted by other ions or chemicals in water, which leads to low sensitivity and unstable signals. Due to the challenges in real applications, commercial ion-selective electrodes are not available for many ions, *e.g.*, phosphate ions.

For voltammetric sensors, the electrode material mainly determines the sensing performance. For real applications, selectivity and durability are its two major limitations. Since many ions and chemicals coexist in the water system, some of them may also be oxidized at a similar potential during the sensing; therefore, the selectivity of the sensor could be influenced, leading to large uncertainties in ion detection. Another issue for the electrode material is poor durability, which decreases the sensitivity of the sensor after use for a period of time. Traditional metal-based electrodes have poor efficiency; therefore, new electrode materials with high catalytic activity, high stability, and low-cost are desired. The integration of nanomaterials with a high effective surface area and high conductivity enhanced the mass transport, improved electrocatalysis, and enabled sensitive detection with a lower detection limit. The application of enzyme into the system also improved the selectivity, but enzymes suffer from poor stability and high cost.

The FET-based sensors offer a rapid response because of the intrinsic high carrier mobility of the semiconducting channel material in the device. The sensing performance of FET-based sensors is influenced by the sensing channel material and the specific probes functionalized on the channel. Selectivity of the ISFET sensors can be improved with the use of various selective membranes from conventional ISEs, which can selectively detect target ion activities. However, the application is limited by the stability of the membrane in an aqueous environment, and some membranes need to be replaced every month, or even sooner. Incorporating nanomaterial into the FET senor significantly improved the sensing performance, especially the sensitivity. The rGO/ferritin FET sensor demonstrated a novel design for detecting water contaminants through the FET platform using semiconducting 2D nanomaterial and specific ion adsorption agents. The selective, sensitive, and stable detection performance suggests a promising future for the FET sensing platform for detecting contamination events in-situ.

To apply nanomaterial-based electronic sensors for the on-site detection of real water samples, the interference from chemical and biological species is a key challenge, as it greatly disturbs the sensing response and thus degrades the sensor sensitivity and selectivity. Some methods have been proposed and developed to address this problem, such as sample pretreatment, the use/development of specific molecular recognition probes (*e.g.*, small organic molecules, proteins, DNA), and integration with microfluidic cells. In addition to the interference issue, reliability, long-term stability, uniformity in the large-scale manufacture, degradation, and false positive all represent great challenges for the commercialization of nanomaterial-based electronic sensors. One future direction to address the uniformity issue is to use printing technology for sensor fabrication. Moreover, research is needed to build a comprehensive calibration model that considers the sensing performance as well as the fabrication uniformity, the intrinsic electronic property of the sensing platform, the ambient environment, and interference from other water components.

Both the detection and the removal/recovery of nutrients from water/wastewater are important. To remove nitrates from water, many denitrification methods have been used, e.g., chemical/biological denitrification, reverse osmosis, nanofiltration, ion exchange, electrodialysis, and electrocatalytic reduction. For the removal of phosphates, common methods include the chemical precipitation method, the electrocoagulation method, and the physiochemical method. For the future development of nutrient sensors, it is highly desirable to design and develop devices that can simultaneously detect and remove the nutrients from aqueous media or wastewater. Another direction is to adapt and integrate the sensor into the existing water treatment system and the nutrient recovery system, providing real-time concentration information to help enhance the efficiency and decrease the cost of the recovery process.

Table 1 Sensing performance and characteristics of potentiometric, voltammetric, and FET sensors for detecting nutrients.

Sensor type	Target	Key sensing element/structure	Working range/LOD	Response time	Advantages	Disadvantages	Ref.
Potentiometric sensor	Nitrate	cyclo [4] pyrrole ether/chemically-modified carbon electrode	1×10^{-5} M	< 10 s	good selectivity, good stability (60 days)		279
		f-MWCNT	5×10^{-7} M	5 s	low LOD, quick response	suffers from interference in high saline level	42
		nanosized carbon black/plasticized PVC	1×10^{-6}-0.1 M LOD: 2.5×10^{-7} M	~4 s	stable potentials, low membrane resistance, quick response	low selectivity	56
	Nitrite	Rh(III)-tetra(t-butylphenylporphyrin)/PVC	5×10^{-6} M	minutes	good selectivity	slow response	74
	Ammonium	methyl methacrylate−decyl methacrylatecopolymer/CNT/PVC	10^{-4}-10^{-3} M LOD: 10^{-7} M	< 10 s		sulfide interference	40
		nonactin/screen-printed paper	10^{-4}-0.1 M	5 s	low power consumption, simple operation, wide linear dynamic ranges	unstable performance	280
	Phosphate	calix[4]arene/PVC	2×10^{-8}-0.1 M	< 8 s	long life (15 weeks), high		103

			LOD: 2×10^{-8} M		selectivity, low LOD, quick response		
		cobalt-based microelectrode	1×10^{-5}-0.1 M LOD: 7.9×10^{-6} M	< 1 min	low LOD	relatively slow response	116
		conducting polymer/poly-TUS membrane	3.2×10^{-5}-0.1 M LOD: 1×10^{-5} M	< 10 s	good selectivity, good sensitivity		281
Voltammetric sensor	Nitrate	L-SCMNPs/carbon paste	6.25×10^{-7} M	minutes	low LOD	interference from nitrite	99
		Cu nanowire	1×10^{-5}-4×10^{-3} M LOD: 1.7×10^{-6} M	seconds	quick response, low LOD, enhanced catalysis	interference from Cl^-, NO_2^-	167
	Nitrite	poly(3,4-ethylenedioxythiophene)/MWCNT	10^{-6} M		good sensitivity, lower operating potential	narrow linear range	282
		n-octylpyridinum hexafluorophosphate/SWCNT	1×10^{-6}-1.2×10^{-2} M LOD: 1×10^{-7} M	seconds	low LOD, wide linear range, high mechanical stability, high selectivity		283
		amine-terminated poly(amidoamine)/MWCNT	5×10^{-6}-1.5×10^{-3} M LOD: 2×10^{-6} M	seconds	low cost, quick response, wide linear range		284
		hexadecyl trimethyl ammonium bromide -GO/MWCNT	5×10^{-6}-8×10^{-4} M LOD: 1.5×10^{-6} M		excellent catalytic properties, high sensitivity	low selectivity	285
		Pd/SWCNT	2×10^{-6}-2.38×10^{-4} M LOD: 2.5×10^{-7} M		low LOD	susceptible to pH, oxygen	183
		SiC NP/amine	3×10^{-7} M	seconds	low cost, long-term application, good operational stability, antifouling properties	poor reproducibility	205
	Ammonium	Cu/polyaniline	1×10^{-6}-1.25×10^{-4} M LOD: 0.5×10^{-6} M	15 s	high selectivity, high sensitivity		286
		MWCNT/Cu	3×10^{-6}-1×10^{-4} M	8 s	quick response, high sensitivity	poor reproducibility	287
		TBCEAT	1×10^{-6}-1×10^{-1} M		high selectivity	need additional agent	137
	Phosphate	bisthiourea/Au electrode	5×10^{-4} M		high selectivity	high LOD, additional agent	209
		activated Ni platform	3×10^{-7} M	seconds	low LOD, good sensitivity, good selectivity		219
		ZrO_2 NP/screen-printed carbon electrode	1.69×10^{-6} M		wide linear range	need reagent	288
FET sensor	Nitrate	o-nitrophenyl octyl ether/PVC	10^{-6} M	seconds	good selectivity, good durability (>3 months)		256
		ENFET	7×10^{-5} M	less than 50s		complicated functionalization	259
		NaR/OFET with extended gate	0 – 4.0×10^{-6} M/45 ppb LOD: 7.3×10^{-7} M	< 20s	highly selective, lower LOD than In-OFET		260
	Nitrite	polysiloxanes membrane	1×10^{-3} – 0.1 M LOD: 2×10^{-4} M		good selectivity to Cl^-, Br^-	high LOD	261
		PVC plasticized membrane	10^{-4}–10^{-1} M		good selectivity		81
	Ammonium	monactin/PVC	6×10^{-4} M	15 ms	quick response	high LOD, short lifetime (1 month)	262
		ZnO nanorod	0.07×10^{-6} - 10^{-3} M LOD: 0.07×10^{-6} M	seconds	good LOD, stable performance for 10 weeks		241
	Phosphate	selective plasticized PVC	1.6×10^{-4} M		high selectivity over much more lipophilic anions, *e.g.* nitrate	high LOD	235
		rGO/ferritin	0.026×10^{-6} M	2 seconds	good LOD, good selectivity over Cl^-, SO_4^{2-} and CO_3^{2-}		267
		PyO/ZnO nanorods/nafion	0.1×10^{-6} –7.0×10^{-3} M	seconds	good selectivity over K^+, SO_4^{2+}, Ca^{2+}, HCO_3^- and TPP, good reproducibility	short lifetime (4 weeks)	242

Acknowledgements

This work was supported by the National Natural Science Foundation of China (21707102) and the 1000 Talents Plan of China. J. Chen acknowledges the financial support from the US National Science Foundation through a GOALI grant (CBET-1606057).

References

1. W. Yao, R. H. Byrne and R. D. Waterbury, *Environ. Sci. Technol.*, 1998, **32**, 2646-2649.
2. M. D. Patey, M. J. A. Rijkenberg, P. J. Statham, M. C. Stinchcombe, E. P. Achterberg and M. Mowlem, *Trac-Trends Anal. Chem.*, 2008, **27**, 169-182.
3. P. Niedzielski, I. Kurzyca and J. Siepak, *Anal. Chim. Acta*, 2006, **577**, 220-224.
4. S. O. Engblom, *Biosens. Bioelectron.*, 1998, **13**, 981-994.
5. A. T. Lawal and S. B. Adeloju, *Biosens. Bioelectron.*, 2013, **40**, 377-384.
6. J. Malan, A. Marouchos, K. Wild-Allen, M. Rayner, P. Ellis and Ieee, in *Oceans*, IEEE, Yeosu, 2012.
7. M. J. Moorcroft, J. Davis and R. G. Compton, *Talanta*, 2001, **54**, 785-803.
8. R. N. Sah, *Commun. Soil Sci. Plant Anal.*, 1994, **25**, 2841-2869.
9. M. Sohail and S. B. Adeloju, *Talanta*, 2016, **153**, 83-98.
10. Q.-H. Wang, L.-J. Yu, Y. Liu, L. Lin, R.-G. Lu, J.-P. Zhu, L. He and Z.-L. Lu, *Talanta*, 2017, **165**, 709-720.
11. C. Warwick, A. Guerreiro and A. Soares, *Biosens. Bioelectron.*, 2013, **41**, 1-11.
12. M. N. R. Sumaiya Islam, Jin-Tae Jeong, Kyeong-Hwan Lee, *J. Biosyst. Eng.*, 2016, **41**, 138-144.
13. J. Langmaier, *Chem. Listy*, 1990, **84**, 697-715.
14. A. S. M. Nor, M. A. M. Yunus, S. W. Nawawi, S. Ibrahim and M. F. a. Rahmat, *Sens. Rev.*, 2015, **35**, 106-115.
15. Y. Zhao, D. Zhao and D. Li, *Int. J. Electrochem. Sci.*, 2015, **10**, 1144-1168.
16. S. Berchmans, T. B. Issa and P. Singh, *Anal. Chim. Acta*, 2012, **729**, 7-20.
17. M. M. Villalba, K. J. McKeegan, D. H. Vaughan, M. F. Cardosi and J. Davis, *J. Mol. Catal. B-Enzym.*, 2009, **59**, 1-8.
18. P. Helmholtz, *Science*, **2**, 182.
19. D. A. Macinnes and M. Dole, *J. Am. Chem. Soc.*, 1930, **52**.
20. E. Lindner and R. E. Gyurcsanyi, *J. Solid State Electrochem.*, 2009, **13**, 51-68.
21. C. Janaky and C. Visy, *Anal. Bioanal. Chem.*, 2013, **405**, 3489-3511.
22. Z. Stefanac and W. Simon, *Chimica*, 1966, **20**, 436-440.
23. L. Michaelis, *Kolloid-Zeitschrift*, 1933, **62**, 2-10.
24. T. Teorell, *J. Gen. Physiol.*, 1936, **19**, 917-927.
25. A. von Ettingshausen and W. Nernst, *Ann. Phys.-Berlin*, 1888, **269**, 474-492.
26. A. v. Ettingshausen and W. Nernst, *Ann. Phys.-Berlin*, 1886, **265**, 343-347.
27. C. J. Coetzee and H. Freiser, *Anal. Chem.*, 1968, **40**, 2071-2071.
28. P. Schulthess, D. Ammann, W. Simon, C. Caderas, R. Stepánek and B. Kräutler, *Helv. Chim. Acta*, 1984, **67**, 1026-1032.
29. E. Graf, J. P. Kintzinger, J. M. Lehn and J. LeMoigne, *J. Am. Chem. Soc.*, 1982, **104**, 1672-1678.
30. D. Kim, I. B. Goldberg and J. W. Judy, *Sens. Actuator B-Chem.*, 2009, **135**, 618-624.
31. J. Chin, C. Walsdorff, B. Stranix, J. Oh, H. J. Chung, S. M. Park and K. Kim, *Angew. Chem. Int. Ed.*, 1999, **38**, 2756.
32. M. Hosseini, S. D. Abkenar, M. R. Ganjali and F. Faridbod, *Mater. Sci. Eng. C-Mater. Biol. Appl.*, 2011, **31**, 428-433.
33. P. Norouzi, M. R. Ganjali, F. Faridbod, S. J. Shahtaheri and H. A. Zamani, *Int. J. Electrochem. Sci.*, 2012, **7**, 2633-2642.
34. A. P. Washe, S. Macho, G. A. Crespo and F. X. Rius, *Anal. Chem.*, 2010, **82**, 8106-8112.
35. S. Chandra, R. Buschbeck and H. Lang, *Talanta*, 2006, **70**, 1087-1093.
36. Y. Kosaki, K. Takano, D. Citterio, K. Suzuki and S. Shiratori, *J. Nanosci. Nanotechnol.*, 2012, **12**, 563.
37. O. Cubuk, M. Altikatoglu, V. Erci, I. Isildak and N. Tinkilic, *Sens. Lett.*, 2013, **11**, 585-590.
38. M. Altikatoglu, E. Karakus, V. Erci, S. Pekyardımcı and I. Isildak, *Artif. Cell. Nanomed. Biotechnol.*, 2013, **41**, 131.
39. J. Ping, Y. Wang, J. Wu and Y. Ying, *Electrochem. Commun.*, 2011, **13**, 1529-1532.
40. R. Athavale, I. Kokorite, C. Dinkel, E. Bakker, B. Wehrli, G. A. Crespo and A. Brand, *Anal. Chem.*, 2015, **87**, 11990.
41. Y. Kan, *Int. J. Electrochem. Sci.*, 2016, **11**, 9928-9940.
42. M. Cuartero, G. A. Crespo and E. Bakker, *Anal. Chem.*, 2015, **87**, 8084-8089.
43. M. Sohail, R. De Marco, K. Lamb and E. Bakker, *Anal. Chim. Acta*, 2012, **744**, 39-44.
44. I. Svancara, K. Kalcher, A. Walcarius and K. Vytras, *Electroanalysis with Carbon Paste Electrodes*, Crc Press, 2012.
45. A. Nezamzadeh-Ejhieh and Z. Nematollahi, *Electrochim. Acta*, 2011, **56**, 8334-8341.
46. K. L. Yong, J. T. Park, K. K. Chang and K. J. Whang, *Anal. Chem.*, 1986, **58**, 2101-2103.
47. G. A. Qureshi and J. Lindquist, *Anal. Chim. Acta*, 1973, **67**, 243-245.
48. B. T. Sun and P. G. Fitch, *Electroanalysis*, 1997, **9**, 494-497.
49. R. S. Hutchins and L. G. Bachas, *Anal. Chem.*, 1995, **67**, 1654-1660.
50. S. C. Kang, K. S. Lee, J. D. Kim and K. J. Kim, *Bull. Korean Chem. Soc.*, 1990, **11**, 124-126.
51. C. Alemán, J. Casanovas, J. Torras, O. Bertrán, E. Armelin, R. Oliver and F. Estrany, *Polymer*, 2008, **49**, 1066-1075.
52. E. M. Bomar, G. S. Owens and G. M. Murray, *Chemosensors*, 2017, **5**, 2.
53. B. Paczosa-Bator, L. Cabaj, R. Piech and K. Skupien, *Analyst*, 2012, **137**, 5272-5277.
54. G. A. Crespo, S. Macho and F. X. Rius, *Anal. Chem.*, 2008, **80**, 1316-1322.
55. W. Tang, J. Ping, K. Fan, Y. Wang, X. Luo, Y. Ying, J. Wu and Q. Zhou, *Electrochim. Acta*, 2012, **81**, 186-190.
56. B. Paczosa-Bator, *Microchim. Acta*, 2014, **181**, 1093-1099.

57. J. M. Dias, M. E. Than, A. Humm, R. Huber, G. P. Bourenkov, H. D. Bartunik, S. Bursakov, J. Calvete, J. Caldeira, C. Carneiro, J. J. G. Moura, I. Moura and M. J. Romão, *Structure*, 1999, **7**, 65-79.
58. W. H. Campbell, *Annu. Rev. Plant Physiol. Plant*, 1999, **50**, 277-303.
59. J. Cooper and T. Cass, *Biosensors*, Oxford University Press, USA, 2004.
60. V. Stewart, *Biochem. Soc. Trans.*, 2003, **31**, 1-10.
61. B. Strehlitz, B. Gründig, K. D. Vorlop, P. Bartholmes, H. Kotte and U. Stottmeister, *Fresenius J. Anal. Chem.*, 1994, **349**, 676-678.
62. R. A. Siddiqui, U. Warneckeeberz, A. Hengsberger, B. Schneider, S. Kostka and B. Friedrich, *J. Bacteriol.*, 1993, **175**, 5867-5876.
63. P. G. Edelman and J. Wang, *Biosensors and chemical sensors: optimizing performance through polymeric materials*, ACS Publications, 1992.
64. E. Malinowska and M. E. Meyerhoff, *Anal. Chim. Acta*, 1995, **300**, 33-43.
65. P. Schulthess, D. Ammann, B. Kraeutler, C. Caderas, R. Stepanek and W. Simon, *Anal. Chem.*, 1985, **57**, 1397-1401.
66. D. Ammann, M. Huser, B. Kräutler, B. Rusterholz, P. Schulthess, B. Lindemann, E. Halder and W. Simon, *Helv. Chim. Acta*, 1986, **69**, 849-854.
67. M. Huser, W. E. Morf, K. Fluri, K. Seiler, P. Schulthess and W. Simon, *Helv. Chim. Acta*, 1990, **73**, 1481-1496.
68. X. Li and D. J. Harrison, *Anal. Chem.*, 1991, **63**, 2168-2174.
69. A. Hodinár and A. Jyo, *Chem. Lett.*, 1988, **17**, 993-996.
70. J. Z. Li, X. C. Wu, R. Yuan, H. G. Lin and R. Q. Yu, *Analyst*, 1994, **119**, 1363-1366.
71. R. Stepánek, B. Kräutler, P. Schulthess, B. Lindemann, D. Ammann and W. Simon, *Anal. Chim. Acta*, 1986, **182**, 83-90.
72. S. Yang and M. E. Meyerhoff, *Electroanalysis*, 2013, **25**, 2579-2585.
73. V. M. Ivanov, *J. Anal. Chem.*, 2004, **59**, 1002-1005.
74. M. Pietrzak and M. E. Meyerhoff, *Anal. Chem.*, 2009, **81**, 3637-3644.
75. C. A. Dalla, B. P. De, G. Forte and F. Y. Mihan, *Chem. Soc. Rev.*, 2010, **39**, 3863-3874.
76. W. Zhang, J. L. Loebach, S. R. Wilson and E. N. Jacobsen, *J. Am. Chem. Soc.*, 1990, **112**, 2801-2803.
77. T. Katasuki, *Chem. Rev.*, 1995, **140**, 189-214.
78. Ł. Górski, A. Matusevich, P. Parzuchowski, I. Łuciuk and E. Malinowska, *Anal. Chim. Acta*, 2010, **665**, 39-46.
79. M. R. Ganjali, F. Mizani and M. Salavati-Niasari, *Anal. Chim. Acta*, 2003, **481**, 85-90.
80. H. R. Zare, F. Memarzadeh, A. Gorji and M. M. Ardakani, *J. Braz. Chem. Soc.*, 2005, **16**, 571-577.
81. W. Wróblewski, Z. Brzózka, D. M. Rudkevich and D. N. Reinhoudt, *Sens. Actuator B-Chem.*, 1996, **37**, 151-155.
82. M. R. Ganjali, S. Shirvani-Arani, P. Norouzi, M. Rezapour and M. Salavati-Niasari, *Microchim. Acta*, 2004, **146**, 35-41.
83. R. Yuan, Y. Chai, D. Liu, D. Gao, J. Li and R. Yu, *Anal. Chem.*, 1993, **65**, 2572-2575.
84. Ł. Górski, A. Saniewska, P. Parzuchowski, M. E. Meyerhoff and E. Malinowska, *Anal. Chim. Acta*, 2005, **551**, 37-44.
85. B. Neel, M. G. Asfhar, G. A. Crespo, M. Pawlak, D. Dorokhin and E. Bakker, *Electroanalysis*, 2014, **26**, 473-480.
86. L. Nunez, X. Ceto, M. I. Pividori, M. V. B. Zanoni and M. del Valle, *Microchem J.*, 2013, **110**, 273-279.
87. E. Pungor, K. Toth and J. Havas, *Microchim. Acta*, 1966, **54**, 689-698.
88. C. Warwick, A. Guerreiro and A. Soares, *Biosens. Bioelectron.*, 2013, **41**, 1.
89. J. K. Tsagatakis, N. A. Chaniotakis and K. Jurkschat, *Helv. Chim. Acta*, 1994, **77**, 2191-2196.
90. S. Sasaki, S. Ozawa, D. Citterio, K. Yamada and K. Suzuki, *Talanta*, 2004, **63**, 131-134.
91. M. M. Benjamin and U. O. Washington, *Water chemistry*, ACS, USA, 2001.
92. V. Zarinskii, L. Shpigun, V. Shkinev, B. Y. Spivakov, V. Trepalina and Y. A. Zolotov, *J. Anal. Chem. USSR*, 1980, **35**, 1376-1380.
93. S. A. Glazier and M. A. Arnold, *Anal. Chem.*, 1988, **60**, 2540-2542.
94. S. A. Glazier and M. A. Arnold, *Anal. Chem.*, 1991, **63**, 754-759.
95. T. Le Goff, J. Braven, L. Ebdon and D. Scholefield, *Anal. Chim. Acta*, 2004, **510**, 175-182.
96. S. Nishizawa, T. Yokobori, R. Kato, K. Yoshimoto, T. Kamaishi and N. Teramae, *Analyst*, 2003, **128**, 663-669.
97. A. S. Adekunle, B. B. Mamba, B. O. Agboola and K. I. Ozoemena, *Int. J. Electrochem. Sci.*, 2011, **6**, 4388-4403.
98. F. Kivlehan, W. J. Mace, H. A. Moynihan and D. W. M. Arrigan, *Anal. Chim. Acta*, 2007, **585**, 154-160.
99. A. Afkhami, T. Madrakian, H. Ghaedi and H. Khanmohammadi, *Electrochim. Acta*, 2012, **66**, 255-264.
100. O. Karagollu, M. Gorur, F. Gode, B. Sennik and F. Yilmaz, *Sens. Actuator B-Chem.*, 2014, **193**, 788-798.
101. A. Kumar, S. Mehtab, U. P. Singh, V. Aggarwal and J. Singh, *Electroanalysis*, 2008, **20**, 1186-1193.
102. M. R. Ganjali, P. Norouzi, M. Ghomi and M. Salavati-Niasari, *Anal. Chim. Acta*, 2006, **567**, 196-201.
103. N. R. Modi, B. Patel, M. B. Patel and S. K. Menon, *Talanta*, 2011, **86**, 121-127.
104. T. Katsu and T. Kayamoto, *Anal. Chim. Acta*, 1992, **265**, 1-4.
105. H. Satoh, Y. Miyazaki, S. Taniuchi, M. Oshiki, R. M. L. D. Rathnayake, M. Takahashi and S. Okabe, *Anal. Sci.*, 2017, **33**, 825-830.
106. M. Benounis, *Sens. Actuator B-Chem.*, 2015, **216**, 57-63.
107. C. Clifton, *Chemosensors*, 2015, **3**, 284-294.
108. E. Khaled, H. N. A. Hassan, A. Girgis and R. Metelka, *Talanta*, 2008, **77**, 737-743.
109. S. Lei, Z. Lei, Y. C. Liu, X. H. Zhou and H. C. Shi, *Sci. China-Chem.*, 2014, **57**, 1283-1290.
110. A. N. Ejhieh and N. Masoudipour, *Anal. Chim. Acta*, 2010, **658**, 68-74.
111. K. Vytras, J. Kalous and J. Jezkova, *Egypt. J. Anal. Chem*, 1997, **6**, 107-123.
112. B. N. Barsoum, W. M. Watson, I. M. Mahdi and E. Khalid, *J. Electroanal. Chem.*, 2004, **567**, 277-281.
113. J. P. Hart and S. A. Wring, *Trac-Trends Anal. Chem.*, 1997, **16**, 89-103.
114. Ł. Tymecki, E. Zwierkowska, S. Głab and R. Koncki, *Sens. Actuator B-Chem.*, 2003, **96**, 482-488.
115. P. G. Veltsistas, M. I. Prodromidis and C. E. Efstathiou, *Anal. Chim. Acta*, 2004, **502**, 15-22.

116. W. H. Lee, Y. Seo and P. L. Bishop, *Sens. Actuator B-Chem.*, 2009, **137**, 121-128.
117. A. T. Lawal and S. B. Adeloju, *Biosens. Bioelectron.*, 2009, **25**, 406-410.
118. S. B. Adeloju and A. Lawal, *Int. J. Environ. Anal. Chem.*, 2005, **85**, 771-780.
119. N. Tamaekong, C. Liewhiran, A. Wisitsoraat and S. Phanichphant, *Sens. Actuator B-Chem.*, 2011, **152**, 155-161.
120. G. L. Turdean, *Int. J. Electrochem.*, 2011, **2011**, 343125.
121. T. Gan, J. Sun, K. Huang, L. Song and Y. Li, *Sens. Actuator B-Chem.*, 2013, **177**, 412-418.
122. F. Winquist, J. Olsson and M. Eriksson, *Anal. Chim. Acta*, 2011, **683**, 192-197.
123. G. Zhang, B. Lu, Y. Wen, L. Lu and J. Xu, *Sens. Actuator B-Chem.*, 2012, **171**, 786-794.
124. A. Ambrosi, C. K. Chua, A. Bonanni and M. Pumera, *Chem. Rev.*, 2014, **114**, 7150-7188.
125. A. Chen and S. Chatterjee, *Chem. Soc. Rev.*, 2013, **42**, 5425-5438.
126. S. K. Vashist, D. Zheng, K. Alrubeaan, J. H. Luong and F. S. Sheu, *Biotechnol. Adv.*, 2011, **29**, 169-188.
127. J. Zhang and C. M. Li, *Chem. Soc. Rev.*, 2012, **41**, 7016-7031.
128. C. Zhu, G. Yang, H. Li, D. Du and Y. Lin, *Anal. Chem.*, 2015, **87**, 230-249.
129. T. Gan and S. Hu, *Microchim. Acta*, 2011, **175**, 1-19.
130. S. Wu, Q. He, C. Tan, Y. Wang and H. Zhang, *Small*, 2013, **9**, 1160-1172.
131. J. N. Tiwari, V. Vij, K. C. Kemp and K. S. Kim, *ACS Nano*, 2016, **10**, 46-80.
132. L. L. Tan, A. Musa and Y. H. Lee, *Sensors*, 2011, **11**, 9344-9360.
133. P. Bertocchi, D. Compagnone and G. Palleschi, *Biosens. Bioelectron.*, 1996, **11**, 1-10.
134. R. C. H. Kwan, P. Y. T. Hon and R. Renneberg, *Sens. Actuator B-Chem.*, 2005, **107**, 616-622.
135. A. K. Abass, J. P. Hart, D. C. Cowell and A. Chappell, *Anal. Chim. Acta*, 1998, **373**, 1-8.
136. J. A. Ribeiro, F. Silva and C. M. Pereira, *Talanta*, 2012, **88**, 54-60.
137. S. Jin, J. S. Lee, Y. Kang, M. Heo, J. H. Shin, G. S. Cha, H. Nam, J. Y. Lee, A. Helal, H.-S. Kim, I. Jeong and J. H. Shim, *Sens. Actuator B-Chem.*, 2015, **207**, 1026-1034.
138. B. Kabagambe, A. Izadyar, S. Amemiya and A. Chem, *Anal. Chem.*, 2012, **84**, 7979.
139. A. Walcarius, V. Vromman and J. Bessiere, *Sens. Actuator B-Chem.*, 1999, **56**, 136-143.
140. M. Faraday, *Phil. Trans. R. Soc. Lond.*, 1834, **124**, 77-122.
141. R. Ahmad, K. S. Bhat, M.-S. Ahn and Y.-B. Hahn, *New J. Chem.*, 2017, **41**, 10992-10997.
142. A. G. Fogg, S. P. Scullion, T. E. Edmonds and B. J. Birch, *Analyst*, 1991, **116**, 573-579.
143. E. Yeager and E. Yeager, *Electrochim. Acta*, 1984, **29**, 1527-1537.
144. O. A. Petrii and T. Y. Safonova, *J. Electroanal. Chem.*, 1992, **331**, 897-912.
145. I. S. D. Silva, W. R. D. Araujo, T. R. L. C. Paixão and L. Angnes, *Sens. Actuator B-Chem.*, 2013, **188**, 94-98.
146. M. Shibata and N. Furuya, *J. Electroanal. Chem.*, 2003, **48**, 3953-3958.
147. G. E. Dima, A. C. A. D. Vooys and M. T. M. Koper, *J. Electroanal. Chem.*, 2003, **554–555**, 15-23.
148. M. Shibata, K. Yoshida and N. Furuya, *J. Electroanal. Chem.*, 1995, **387**, 143-145.
149. N. G. Carpenter and D. Pletcher, *Anal. Chim. Acta*, 1995, **317**, 287-293.
150. D. Pletcher and Z. Poorabedi, *Electrochim. Acta*, 1979, **24**, 1253-1256.
151. B. P. Dash and S. Chaudhari, *Water Res.*, 2005, **39**, 4065-4072.
152. V. Mori and M. Bertotti, *Anal. Lett.*, 1999, **32**, 25-37.
153. D. Kim, I. B. Goldberg and J. W. Judy, *Analyst*, 2007, **132**, 350-357.
154. X. Chen, F. Wang and Z. Chen, *Anal. Chim. Acta*, 2008, **623**, 213-220.
155. J. D. Genders, D. Hartsough and D. T. Hobbs, *J. Appl. Electrochem.*, 1996, **26**, 1-9.
156. M. J. Moorcroft, L. Nei, J. Davis and R. G. Compton, *Anal. Lett.*, 2000, **33**, 3127-3136.
157. M. E. Bodini and D. T. Sawyer, *Anal. Chem.*, 1977, **49**, 485-489.
158. K. Soropogui, M. Sigaud and O. Vittori, *Electroanalysis*, 2010, **18**, 2354-2360.
159. M. B. Gumpu, N. Nesakumar, B. L. Ramachandra and J. B. B. Rayappan, *J. Anal. Chem.*, 2017, **72**, 316-326.
160. W. Lijinsky, *Chemistry and biology of N-nitroso compounds*, Cambridge University Press, London, 1992.
161. S. I. R. Malha, J. Mandli, A. Ourari and A. Amine, *Electroanalysis*, 2013, **25**, 2289–2297.
162. F. Bouamrane, A. Tadjeddine, J. E. Butler, R. Tenne and C. Lévy-Clément, *J. Electroanal. Chem.*, 1996, **405**, 95-99.
163. M. Zhou and S. Guo, *ChemCatChem*, 2015, **7**, 2744-2764.
164. J. Xu, Y. Wang and S. Hu, *Microchim. Acta*, 2017, **184**, 1-44.
165. A. S. Lima, M. O. Salles, T. L. Ferreira, T. R. L. C. Paixão and M. Bertotti, *Electrochim. Acta*, 2012, **78**, 446-451.
166. D. Reyter, M. Odziemkowski, D. BéLanger and L. Roué, *J. Electrochem. Soc.*, 2007, **154**, K36-K44.
167. A. M. Stortini, L. M. Moretto, A. Mardegan, M. Ongaro and P. Ugo, *Sens. Actuator B-Chem.*, 2015, **207**, 186-192.
168. B. Hafezi and M. R. Majidi, *Anal. Methods*, 2013, **5**, 3552-3556.
169. F. Patolsky, E. Katz, V. Heleg‐Shabtai and I. Willner, *Chem.-Eur. J.*, 2015, **4**, 1068-1073.
170. L. M. Moretto, P. Ugo, M. Zanata, P. Guerriero and C. R. Martin, *Anal. Chem.*, 1998, **70**, 2163-2166.
171. S. A. Glazier, E. R. C. And and W. H. Campbell, *Anal. Chem.*, 1998, **70**, 1511-1515.
172. K. Takayama, K. Kano and T. Ikeda, *Chem. Lett.*, 1996, **25**, 1009-1010.
173. S. M. da Silva and L. H. Mazo, *Electroanalysis*, 1998, **10**, 1200-1203.
174. C. Milhano and D. Pletcher, *J. Electroanal. Chem.*, 2008, **614**, 24-30.
175. F. Armijo, M. C. Goya, M. Reina, M. J. Canales, M. C. Arévalo and M. J. Aguirre, *J. Mol. Catal. A-Chem.*, 2007, **268**, 148-154.
176. R. Ahmad, M.-S. Ahn and Y.-B. Hahn, *Adv. Mater. Interfaces*, 2017, **4**, 1700691.

177. P. Kalimuthu and S. A. John, *Electrochem. Commun.*, 2009, **11**, 1065-1068.
178. J. R. C. Rocha, L. Kosminsky, T. R. L. C. Paixão and M. Bertotti, *Electroanalysis*, 2015, **13**, 155-160.
179. N. SpãTaru, T. N. Rao, D. A. Tryk and A. Fujishima, *J. Electrochem. Soc.*, 2001, **148**, E112-E117.
180. I. Švancara, K. Vytřas, J. Barek and J. Zima, *Rev. Anal. Chem.*, 2001, **31**, 311-345.
181. W. H. Lee, D. G. Wahman and J. G. Pressman, *Sens. Actuator B-Chem.*, 2013, **188**, 1263-1269.
182. M. Parsaei, Z. Asadi and S. Khodadoust, *Sens. Actuator B-Chem.*, 2015, **220**, 1131-1138.
183. X.-H. Pham, C. A. Li, K. N. Han, H.-N. Buu-Chau, L. Thanh-Hai, E. Ko, J. H. Kim and G. H. Seong, *Sens. Actuator B-Chem.*, 2014, **193**, 815-822.
184. Y. Zhang, J. Yin, K. Wang, P. Chen and L. Ji, *Sens. Actuator B-Chem.*, 2013, **185**, 602-607.
185. Z. Wang, F. Liao, T. Guo, S. Yang and C. Zeng, *J. Electroanal. Chem.*, 2012, **664**, 135-138.
186. S. Yang, X. Liu, X. Zeng, B. Xia, J. Gu, S. Luo, N. Mai and W. Wei, *Sens. Actuator B-Chem.*, 2010, **145**, 762-768.
187. Y. Cui, C. Yang, W. Zeng, M. Oyama, W. Pu and J. Zhang, *Anal. Sci.*, 2007, **23**, 1421-1425.
188. S. Wang, Y. Yin and X. Lin, *Electrochem. Commun.*, 2004, **6**, 259-262.
189. G. Xu, S. Liang, J. Fan, G. Sheng and X. Luo, *Microchim. Acta*, 2016, **183**, 2031-2037.
190. N. Tian, Z.-Y. Zhou and S.-G. Sun, *J. Phys. Chem. C*, 2008, **112**, 19801-19817.
191. X. Xiao, X. Liu, H. Zhao, D. Chen, F. Liu, J. Xiang, Z. Hu and Y. Li, *Adv. Mater.*, 2012, **24**, 5762-5766.
192. D. Koziej, M. D. Rossell, B. Ludi, A. Hintennach, P. Novák, J.-D. Grunwaldt and M. Niederberger, *Small*, 2011, **7**, 377-387.
193. P. Kalita, J. Singh, M. Kumar Singh, P. R. Solanki, G. Sumana and B. D. Malhotra, *Appl. Phys. Lett.*, 2012, **100**, 093702.
194. C. Batchelor-McAuley, G. G. Wildgoose, R. G. Compton, L. Shao and M. L. H. Green, *Sens. Actuator B-Chem.*, 2008, **132**, 356-360.
195. M. Li, F. Gao, P. Yang, L. Wang and B. Fang, *Surf. Sci.*, 2008, **602**, 151-155.
196. X. Sun, S. Guo, Y. Liu and S. Sun, *Nano Lett.*, 2012, **12**, 4859-4863.
197. H. Teymourian, A. Salimi and S. Khezrian, *Biosens. Bioelectron.*, 2013, **49**, 1-8.
198. V. Mani, A. P. Periasamy and S.-M. Chen, *Electrochem. Commun.*, 2012, **17**, 75-78.
199. X. R. Li, J. Liu, F. Y. Kong, X. C. Liu, J. J. Xu and H. Y. Chen, *Electrochem. Commun.*, 2012, **20**, 109-112.
200. X. Wang, L. I. Hui, W. U. Min, G. E. Shu-Li, Y. Zhu, Q. J. Wang, H. E. Ping-Gang and Y. Z. Fang, *Chin. J. Anal. Chem.*, 2013, **41**, 1232-1237.
201. C.-J. Shih, G. L. C. Paulus, Q. H. Wang, Z. Jin, D. Blankschtein and M. S. Strano, *Langmuir*, 2012, **28**, 8579-8586.
202. H. L. Ke, J. Lin, Y. Ye, W. J. Wu, H. H. Lin, H. Wei, M. Huang, D. W. Chang, C. P. Dinney and X. Wu, *J. Mater. Chem.*, 2011, **21**, 8032-8037.
203. Y. Fan, K. J. Huang, D. J. Niu, C. P. Yang and Q. S. Jing, *Electrochim. Acta*, 2011, **56**, 4685-4690.
204. F. Zhang, Y. Li, Y.-e. Gu, Z. Wang and C. Wang, *Microchim. Acta*, 2011, **173**, 103-109.
205. A. Salimi, M. Kurd, H. Teymourian and R. Hallaj, *Sens. Actuator B-Chem.*, 2014, **205**, 136-142.
206. Y. Zhang, J. Yin, K. Wang, P. Chen and L. Ji, *J. Appl. Polym. Sci.*, 2013, **128**, 2971-2976.
207. D. Quan and S. Woonsup, *Sensors*, 2010, **10**, 6241-6256.
208. W. Suginta, P. Khunkaewla and A. Schulte, *Chem. Rev.*, 2013, **113**, 5458-5479.
209. H. Aoki, K. Hasegawa, K. Tohda and Y. Umezawa, *Biosens. Bioelectron.*, 2003, **18**, 261-267.
210. P. D. Beer, M. G. B. Drew, A. R. Graydon, D. K. Smith and S. E. Stokes, *J. Chem. Soc.-Dalton Trans.*, 1995, **3**, 403-408.
211. L. Gilbert, A. T. Jenkins, S. Browning and J. P. Hart, *Anal. Biochem.*, 2009, **393**, 242-247.
212. S. Cinti, D. Talarico, G. Palleschi, D. Moscone and F. Arduini, *Anal. Chim. Acta*, 2016, **919**, 78-84.
213. J. Jońca, F. V. León, D. Thouron, A. Paulmier, M. Graco and V. Garçon, *Talanta*, 2011, **87**, 161-167.
214. Y. Udnan, I. D. Mckelvie, M. R. Grace, J. Jakmunee and K. Grudpan, *Talanta*, 2005, **66**, 461-466.
215. J. C. Quintana, L. Idrissi, G. Palleschi, P. Albertano, A. Amine, R. M. El and D. Moscone, *Talanta*, 2004, **63**, 567-574.
216. M. T. Rojas, R. Koeniger, J. F. Stoddart and A. E. Kaifer, *J. Am. Chem. Soc.*, 1995, **117**, 336-343.
217. D. Midgley, *Ion-Selective Electrode Reviews*, Elsevier, 1986.
218. Z. Zou, J. Han, A. Jang, P. L. Bishop and C. H. Ahn, *Biosens. Bioelectron.*, 2007, **22**, 1902-1907.
219. W.-L. Cheng, J.-W. Sue, W.-C. Chen, J.-L. Chang and J.-M. Zen, *Anal. Chem.*, 2010, **82**, 1157-1161.
220. L. A. Godínez, J. Lin, M. Muñoz, A. W. Coleman and A. E. Kaifer, *Electroanalysis*, 1996, **8**, 1072-1074.
221. A. Berduque, G. Herzog, Y. E. Watson, D. W. M. Arrigan, J.-C. Moutet, O. Reynes, G. Royal and E. Saint-Aman, *Electroanalysis*, 2005, **17**, 392-399.
222. C. Storer, Z. Coldrick, D. Tate, J. Donoghue and B. Grieve, *Sensors*, 2018, **18**, 531.
223. G. Zhou, J. Chang, S. Cui, H. Pu, Z. Wen and J. Chen, *ACS Appl. Mater. Interfaces*, 2014, **6**, 19235-19241.
224. Y. Chen, R. Ren, H. Pu, J. Chang, S. Mao and J. Chen, *Biosens. Bioelectron.*, 2017, **89**, 505-510.
225. J. Chang, G. Zhou, E. R. Christensen, R. Heideman and J. Chen, *Anal. Bioanal. Chem.*, 2014, **406**, 3957-3975.
226. C. Wang, H. Dong, W. Hu, Y. Liu and D. Zhu, *Chem. Rev.*, 2012, **112**, 2208-2267.
227. G. E. Andredakis, E. A. Moschou, K. Matthaiou, G. E. Froudakis and N. A. Chaniotakis, *Anal. Chim. Acta*, 2001, **439**, 273-280.
228. Y. P. Ling, M. I. Syono and L. Y. Heng, *Malaysian Journal of Chemistry*, 2009, **11**, 64-72.
229. J. Artigas, A. Beltran, C. Jimenez, A. Baldi, R. Mas, C. Dominguez and J. Alonso, *Comput. Electron. Agric.*, 2001, **31**, 281-293.
230. S. D. T. Kelly, N. K. Suryadevara and S. C. Mukhopadhyay, *IEEE Sens. J.*, 2013, **13**, 3846-3853.
231. Y. Alifragis, A. Volosirakis, N. A. Chaniotakis, G. Konstantinidis, E. Iliopoulos and A. Georgakilas, *Phys. Status Solidi A-Appl. Mat.*, 2007, **204**, 2059-2063.
232. N. K. Madzhi, A. b. Ahmad, L. Y. Khuan, R. A. Rani, M. I. Syono and F. Abdullah, in *International Conference on Nanoscience and Nanotechnology (NANO-SciTech 2008)* ed. M. S. Rusop, T, AIP, Selangor, Malaysia vol. 1136, pp. 801-806.

233. A. Beltran, J. Artigas, C. Jimenez, R. Mas, J. Bartroli and J. Alonso, *Electroanalysis*, 2002, **14**, 213-220.
234. L. Y. Heng, S. Alva and M. Ahmad, *Sens. Actuator B-Chem.*, 2004, **98**, 160-165.
235. M. M. G. Antonisse, B. H. M. Snellink-Ruel, I. Yigit, J. F. J. Engbersen and D. N. Reinhoudt, *J. Org. Chem.*, 1997, **62**, 9034-9038.
236. N. F. Nazarudin, M. A. M. Noor, N. Z. A. Rashid, G. Witjaksono and N. A. Nayan, in *IEEE International conference on Biomedical Engineering and Sciences*, IEEE, Miri, Malaysia, 2014, vol. 43, pp. 154-158.
237. S. Mao, J. Chang, G. Zhou and J. Chen, *Small*, 2015, **11**, 5336-5359.
238. J. Chang, G. Zhou, X. Gao, S. Mao, S. Cui, L. E. Ocola, C. Yuan and J. Chen, *Sensing and Bio-Sensing Research*, 2015, **5**, 97-104.
239. S. Mao, J. Chang, H. Pu, G. Lu, Q. He, H. Zhang and J. Chen, *Chem. Soc. Rev.*, 2017, **46**, 6872-6904.
240. J. Chang, S. Mao, Y. Zhang, S. Cui, G. Zhou, X. Wu, C. H. Yang and J. Chen, *Nanoscale*, 2013, **5**, 3620-3626.
241. R. Ahmad, N. Tripathy, M. Y. Khan, K. S. Bhat, M.-s. Ahn and Y.-B. Hahn, *RSC Adv.*, 2016, **6**, 54836-54840.
242. R. Ahmad, M.-S. Ahn and Y.-B. Hahn, *J. Colloid Interface Sci.*, 2017, **498**, 292-297.
243. M. Allen, E. M. Sabio, X. Qi, B. Nwengela, M. S. Islam and F. E. Osterloh, *Langmuir*, 2008, **24**, 7031-7037.
244. L. Luo, J. Jie, W. Zhang, Z. He, J. Wang, G. Yuan, W. Zhang, L. C. M. Wu and S.-T. Lee, *Appl. Phys. Lett.*, 2009, **94**, 193101.
245. R. Ahmad, T. Mahmoudi, M.-S. Ahn and Y.-B. Hahn, *Biosens. Bioelectron.*, 2018, **100**, 312-325.
246. R. A. Villamizar, A. Maroto, F. X. Rius, I. Inza and M. J. Figueras, *Biosens. Bioelectron.*, 2008, **24**, 279-283.
247. C. García-Aljaro, L. N. Cella, D. J. Shirale, M. Park, F. J. Muñoz, M. V. Yates and A. Mulchandani, *Biosens. Bioelectron.*, 2010, **26**, 1437-1441.
248. E. S. Forzani, X. Li, P. Zhang, N. Tao, R. Zhang, I. Amlani, R. Tsui and L. A. Nagahara, *Small*, 2006, **2**, 1283-1291.
249. B. Zhan, C. Li, J. Yang, G. Jenkins, W. Huang and X. Dong, *Small*, 2014, **10**, 4042-4065.
250. L. Li, Y. Yu, G. J. Ye, Q. Ge, X. Ou, H. Wu, D. Feng, X. H. Chen and Y. Zhang, *Nat. Nanotechnol.*, 2014, **9**, 372-377.
251. G. Zhou, H. Pu, J. Chang, X. Sui, S. Mao and J. Chen, *Sens. Actuator B-Chem.*, 2018, **257**, 214-219.
252. V. Rocher, N. Jaffrezicrenault, H. Perrot, Y. Chevalier and P. Leperchec, *Anal. Chim. Acta*, 1992, **256**, 251-255.
253. J. Gavora, D. Gerson, J. Luong, A. Storer and J. Woodley, *Biotechnology research and applications*, Springer Science & Business Media, 2012.
254. S.-i. Wakida, T. Okumura, Y. Shibutani and H. Liu, *Sens. Mater.*, 2007, **19**, 235-247.
255. M. M. G. Antonisse, R. J. W. Lugtenberg, R. J. M. Egberink, J. F. J. Engbersen and D. N. Reinhoudt, *Anal. Chim. Acta*, 1996, **332**, 123-129.
256. W. Wróblewski, M. Chudy and A. Dybko, *Anal. Chim. Acta*, 2000, **416**, 97-104.
257. S. J. Birrell and J. W. Hummel, *Trans. ASAE*, 2000, **43**, 197-206.
258. M. Myers, A. Podolska, T. Pope, F. Khir, B. Nener, M. Baker and G. Parish, *Proceedings IMCS 2012*, 2012, 671-673.
259. M. Zayats, A. B. Kharitonov, E. Katz and I. Willner, *Analyst*, 2001, **126**, 652-657.
260. T. Minami, Y. Sasaki, T. Minamiki, S.-i. Wakida, R. Kurita, O. Niwa and S. Tokito, *Biosens. Bioelectron.*, 2016, **81**, 87-91.
261. M. M. G. Antonisse, B. H. M. Snellink-Ruel, J. F. J. Engbersen and D. N. Reinhoudt, *J. Chem. Soc.-Perkin Trans. 2*, 1998, 773-778.
262. Y.-B. Hahn, R. Ahmad and N. Tripathy, *Chem. Commun.*, 2012, **48**, 10369-10385.
263. U. Oesch, S. Caras and J. Janata, *Anal. Chem.*, 1981, **53**, 1983-1986.
264. N. Kazanskaya, A. Kukhtin, M. Manenkova, N. Reshetilov, L. Yarysheva, O. Arzhakova, A. Volynskii and N. Bakeyev, *Biosens. Bioelectron.*, 1996, **11**, 253-261.
265. A. Senillou, N. Jaffrezic-Renault, C. Martelet and F. Griffe, *Mater. Sci. Eng. C-Biomimetic Supramol. Syst.*, 1998, **6**, 59-63.
266. J. H. Liu, Y. Masuda, E. Sekido, S. I. Wakida and K. Hiiro, *Anal. Chim. Acta*, 1989, **224**, 145-151.
267. S. Mao, H. Pu, J. Chang, X. Sui, G. Zhou, R. Ren, Y. Chen and J. Chen, *Environ.-Sci. Nano*, 2017, **4**, 856-863.
268. S. Mao, K. Yu, J. Chang, D. A. Steeber, L. E. Ocola and J. Chen, *Sci. Rep.*, 2013, **3**, 1696.
269. Z. Bo, S. Mao, ZJ. Han, K. Cen, J. Chen and KK. Ostrikov, *Chem. Soc. Rev.*, 2015, **44**, 2108-2121.
270. S. Cui, S. Mao, G. Lu and J. Chen, *J. Phys. Chem. Lett.*, 2013, **4**, 2441-2454.
271. S. Mao and J. Chen, *J. Mater. Res.*, 2017, **32**, 2954-2965.
272. K. Chen, G. Lu, J. Chang, S. Mao, K. Yu, S. Cui and J. Chen, *Anal. Chem.*, 2012, **84**, 4057-4062.
273. S. Mao, G. Lu and J. Chen, *J. Mater. Chem. A*, 2014, **2**, 5573-5579.
274. A. Maity, X. Sui, C. R. Tarman, H. Pu, J. Chang, G. Zhou, R. Ren, S. Mao and J. Chen, *ACS Sensors*, 2017, **2**, 1653-1661.
275. K. I. Bolotin, K. J. Sikes, Z. Jiang, M. Klima, G. Fudenberg, J. Hone, P. Kim and H. L. Stormer, *Solid State Commun.*, 2008, **146**, 351-355.
276. J. Hwang, D. S. Kim, D. Ahn and S. W. Hwang, *Jpn. J. Appl. Phys.*, 2009, **48**, 06FD08.
277. S. Hong and S. Myung, *Nat. Nanotechnol.*, 2007, **2**, 207-208.
278. R. K. Joshi, H. Gomez, F. Alvi and A. Kumar, *J. Phys. Chem. C*, 2010, **114**, 6610-6613.
279. N. Alizadeh and S. Nabavi, *Sens. Actuator B-Chem.*, 2014, **205**, 127-135.
280. T. Guinovart, A. J. Bandodkar, J. R. Windmiller, F. J. Andrade and J. Wang, *Analyst*, 2013, **138**, 7031-7038.
281. J. Kim, D. M. Kang, S. C. Shin, M. Y. Choi, J. Kim, S. S. Lee and J. S. Kim, *Anal. Chim. Acta*, 2008, **614**, 85-92.
282. C. Y. Lin, V. S. Vasantha and K. C. Ho, *Sens. Actuator B-Chem.*, 2009, **140**, 51-57.
283. L. Zhou, J.-P. Wang, L. Gai, D.-J. Li and Y.-B. Li, *Sens. Actuator B-Chem.*, 2013, **181**, 65-70.
284. N. Zhu, Q. Xu, S. Li and H. Gao, *Electrochem. Commun.*, 2009, **11**, 2308-2311.
285. Y. J. Yang and W. Li, *Biosens. Bioelectron.*, 2014, **56**, 300-306.
286. M. Zhybak, V. Beni, M. Y. Vagin, E. Dempsey, A. P. F. Turner and Y. Korpan, *Biosens. Bioelectron.*, 2016, **77**, 505-511.
287. F. Valentini, V. Biagiotti, C. Lete, G. Palleschi and J. Wang, *Sens. Actuator B-Chem.*, 2007, **128**, 326-333.
288. W.-L. Cheng, J.-L. Chang, Y.-L. Su and J.-M. Zen, *Electroanalysis*, 2013, **25**, 2605-2612.

TOC